

## Structural Characterization of Cranberry Arabinoxyloglucan Oligosaccharides

Kimberly M. Auker,<sup>†</sup> Christina M. Coleman,<sup>\*,†,‡,§</sup> Mei Wang,<sup>†,‡,§</sup> Bharathi Avula,<sup>‡</sup> Susanna L. Bonnet,<sup>§</sup> Lindsey L. Kimble,<sup>‡</sup> Bridget D. Mathison,<sup>‡</sup> Boon P. Chew,<sup>‡</sup> and Daneel Ferreira<sup>\*,†,‡,§</sup>

<sup>†</sup>Department of BioMolecular Sciences, Division of Pharmacognosy, and the Research Institute of Pharmaceutical Sciences, School of Pharmacy, University of Mississippi, University, Mississippi 38677, United States

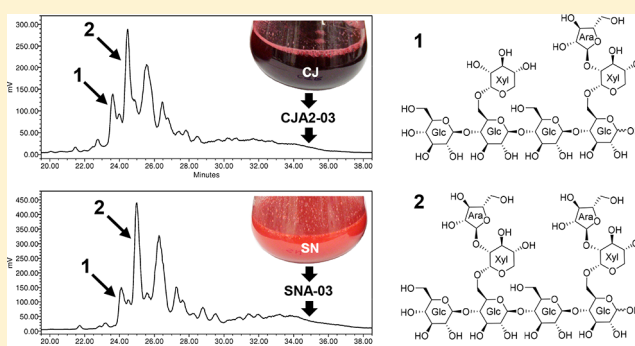
<sup>‡</sup>National Center for Natural Products Research and the Research Institute for Pharmaceutical Sciences, School of Pharmacy, University of Mississippi, University, Mississippi 38677, United States

<sup>§</sup>Department of Chemistry, University of the Free State, 205 Nelson Mandela Drive, Bloemfontein, 9301, South Africa

<sup>‡</sup>School of Food Science, Washington State University, Pullman, Washington 99164-6376, United States

### Supporting Information

**ABSTRACT:** Cranberry (*Vaccinium macrocarpon*) products are widely available in North American food, juice, and dietary supplement markets. The use of cranberry is popular for the prevention of urinary tract infections (UTIs) and other reported health benefits. Preliminary findings by our research group indicate that arabinoxyloglucan oligosaccharides are present in cranberry products and may contribute to the antiadhesion properties of urine produced after cranberry consumption, but relatively little is known regarding the oligosaccharide components of cranberry. This report describes the isolation from two cranberry sources and the complete structure elucidation of two arabinoxyloglucan oligosaccharides through the use of carbohydrate-specific NMR spectroscopic and chemical derivatization methods. These compounds were identified as the heptasaccharide  $\beta$ -D-glucopyranosyl-(1 $\rightarrow$ 4)-[ $\alpha$ -D-xylopyranosyl-(1 $\rightarrow$ 6)]- $\beta$ -D-glucopyranosyl-(1 $\rightarrow$ 4)- $\beta$ -D-glucopyranosyl-(1 $\rightarrow$ 4)-[ $\alpha$ -L-arabinofuranosyl-(1 $\rightarrow$ 2)]- $\alpha$ -D-xylopyranosyl-(1 $\rightarrow$ 6)]- $\beta$ -D-glucopyranose (**1**) and the octasaccharide  $\beta$ -D-glucopyranosyl-(1 $\rightarrow$ 4)-[ $\alpha$ -L-arabinofuranosyl-(1 $\rightarrow$ 2)]- $\alpha$ -D-xylopyranosyl-(1 $\rightarrow$ 6)]- $\beta$ -D-glucopyranosyl-(1 $\rightarrow$ 4)- $\beta$ -D-glucopyranosyl-(1 $\rightarrow$ 4)-[ $\alpha$ -L-arabinofuranosyl-(1 $\rightarrow$ 2)]- $\alpha$ -D-xylopyranosyl-(1 $\rightarrow$ 6)]- $\beta$ -D-glucopyranose (**2**). Selected fractions and the isolated compounds were subjected to antimicrobial, cell viability, and *E. coli* antiadhesion assays. Results indicated that enriched fractions and purified compounds lacked antimicrobial and cytotoxic effects, supporting the potential use of such compounds for disease prevention without the risk for resistance development. Preliminary antiadhesion results indicated that mixtures of oligosaccharides exhibited greater antiadhesion properties than purified fractions or pure compounds. The potential use of cranberry oligosaccharides for the prevention of UTIs warrants continued investigations of this complex compound series.



Products prepared from the American cranberry [*Vaccinium macrocarpon* Ait., (Ericaceae)] are widely available and of significant commercial interest in food, juice, and dietary supplement markets.<sup>1</sup> Cranberry products are popularly used for a variety of reported health benefits, but most notably for the promotion of urinary tract health and for the prevention of urinary tract infections (UTIs).<sup>2,3</sup> Compounds known to be responsible for the aroma, flavor, color, processing stability, and antioxidant properties of cranberry include terpenes, aromatic acids, monosaccharides, simple phenolics, polyphenols, and a wide variety of flavonoids.<sup>2,3</sup> High molecular weight nondialyzable materials (NDM) derived from cranberry products have also been reported and have been found to have various bioactivities including the inhibition of adhesion by bacteria<sup>4–9</sup> and viruses,<sup>10</sup> inhibition of bacterial biofilm

formation,<sup>9</sup> and anti-inflammatory effects on human immune components.<sup>11</sup> To date, however, the exact composition of the NDM cranberry fractions used in these studies has not been fully characterized.<sup>4–11</sup>

The literature has been dominated since 1998 by the hypothesis that polymeric flavan-3-ols known as proanthocyanidins (PACs) are the primary components responsible for the antiadhesion properties of cranberry products and of urine after cranberry consumption.<sup>12,13</sup> Findings by our research group, however, indicate that arabinoxyloglucan oligosacchar-

**Special Issue:** Special Issue in Honor of Drs. Rachel Mata and Barbara Timmermann

**Received:** December 9, 2018

ides are an additional class of antiadhesive compounds found in cranberry products and are likely to contribute to the antiadhesion properties of urine produced after cranberry consumption.<sup>14,15</sup> This oligosaccharide hypothesis has been supported by reports that cranberry fractions enriched in xyloglucan oligosaccharides are able to prevent bacterial adhesion and interfere with biofilm formation.<sup>16,17</sup> Recent analyses of cranberry NDM have indicated the presence of xyloglucan oligosaccharides in addition to PACs and suggest that relatively low molecular weight oligosaccharides may form microaggregates in solution that are retained by the dialysis membranes used in the preparation of such materials.<sup>9</sup> These findings shed new light on the original reports concerning cranberry NDM<sup>4,5</sup> that later led to studies that identified PACs as the antiadhesive constituents of cranberry<sup>12,13</sup> and make it clear that more must be known about cranberry oligosaccharides as they relate to the biological properties of cranberry products.

The carbohydrate composition of cranberry products has not been well characterized, and nothing was known regarding cranberry oligosaccharides when this project was initiated in 2011. The gel-forming characteristics of cranberries, as exhibited by the classic cranberry sauce, led to early structural investigations of complex carbohydrates such as pectins and other cell-wall-associated insoluble polysaccharides related to cellulose.<sup>18</sup> Studies on soluble carbohydrates have been limited to mono- and disaccharides with the use of standards for comparisons.<sup>19</sup> Metabolomics studies on cranberry chemical composition with regard to carbohydrates have been limited by the availability of known compound databases and by the suitability of analysis and detection methods for complex carbohydrates.<sup>20</sup> Recent investigations of the oligosaccharide profile of cranberry have used a pectinase treatment of cranberry hulls followed by various separation methods and chemical analyses of the resulting fractions with MALDI-TOF/TOF MS/MS characterization of the xyloglucan portion of this material.<sup>16,17,21,22</sup> These reports propose arabinoxyloglucan structures similar to that of the octasaccharide isolated from porcine urine after cranberry consumption,<sup>14,15</sup> but do not provide full structural characterization of isolated compounds.

Our research group has found that the oligosaccharide profile of cranberry materials is similar to that found in urine after cranberry consumption, indicating that a portion of the cranberry oligosaccharide series may be excreted intact into urine and thereby contribute to the ability of cranberry materials to prevent UTIs.<sup>14,15</sup> Excretion of these compounds by the fecal route is also likely, and beneficial gut microbes have been identified that are able to ferment cranberry xyloglucan mixtures.<sup>22</sup> This class of compounds may therefore also contribute to various gut-associated health benefits attributed to cranberry materials such as systemic anti-inflammatory effects.<sup>23</sup> Full characterization of all components of this complex mixture of cranberry oligosaccharides will therefore be necessary to fully investigate the metabolism and excretion profiles of these compounds in mammalian systems and to further investigate their biological properties. Toward this end, this report describes the isolation of two arabinoxyloglucan oligosaccharides from two distinct sources of cranberry material and provides details for the complete structure elucidation of both compounds using extensive NMR data analyses in combination with a series of optimized chemical derivatization methods. Selected fractions and the isolated compounds were subjected to antimicrobial and cell

viability assays and to a P-fimbriated *Escherichia coli* uroepithelial cell (EC-UEC) antiadhesion assay that was under development at the time of this project.

## RESULTS AND DISCUSSION

**Isolation.** The oligosaccharides **1** and **2** were isolated from the aqueous extracts of two different cranberry materials, SN and CJ (Figure S1, Supporting Information). These materials were obtained from two separate suppliers and differed in that the SN material was a cranberry fruit powder, while the CJ material was a juice powder. The initial appearance of these parent materials in aqueous solution differed markedly (Figure S1, Supporting Information), but later fractions and sub-fractions behaved similarly and appeared to contain similar constituents as determined by NMR data and various chemical analyses (data not shown). Both yielded oligosaccharide mixtures with similar profiles as visible by HPLC and <sup>1</sup>H NMR spectroscopy (Figures 1 and 2; Figures S5, S6, S9, and

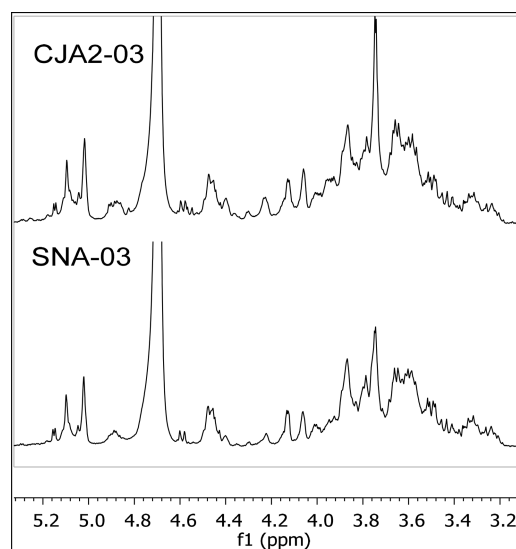


**Figure 1.** <sup>1</sup>H NMR spectra of cranberry oligosaccharide fractions SNA-03 and CJA2-03 (D<sub>2</sub>O, 400 MHz). Resonances do not appear outside of the region shown. See Figure S9 (Supporting Information) for full spectra and expansions. Both of these materials are similar to the CJA1-02 material discussed in the companion manuscript<sup>15</sup> (Figure S7, Supporting Information).

S10, Supporting Information), and both parent materials yielded the same two oligosaccharides via parallel purification methods (Figures S10–S13, Supporting Information).

Compounds **1** and **2** were obtained via sequential fractionation and purification steps, including Sephadex LH-20 size exclusion chromatography and preparative HPLC with C<sub>18</sub> and polyamine stationary phases (Figures S2–S6, S11–S13 and Tables S1 and S2, Supporting Information). Selected Sephadex LH-20 fractions were determined to contain oligosaccharides based on <sup>1</sup>H NMR spectroscopic (Figure 1) and chromatographic data and comparisons to previously characterized material, including CJA1-02 and known monosaccharides (Figures S3–S10, Supporting Information).<sup>15</sup> Fractions SNA-02 and CJA2-02 contained glycans with arabinosyl and glucosyl subunits, as determined by 1D and HSQC NMR data (Figure S10, Supporting Information), but material from these fractions could not be sufficiently purified with the resources available for this study (Figures S5 and S6,

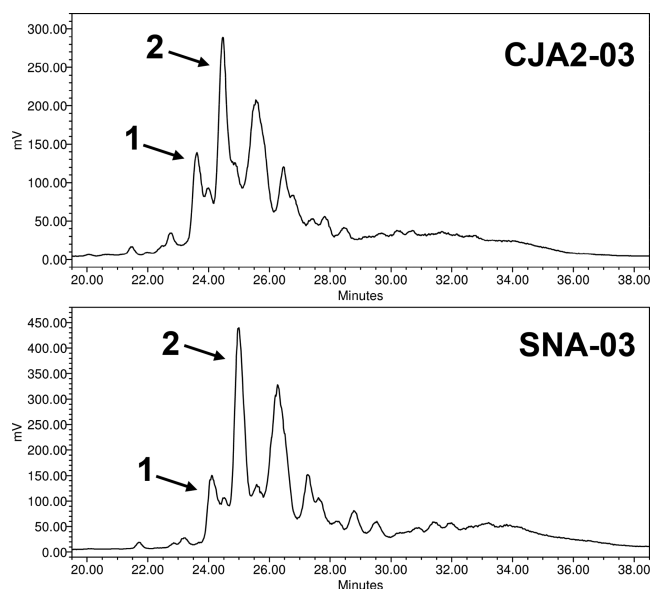
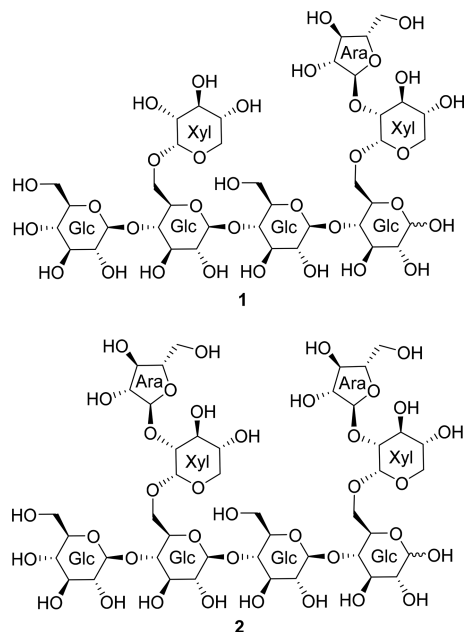
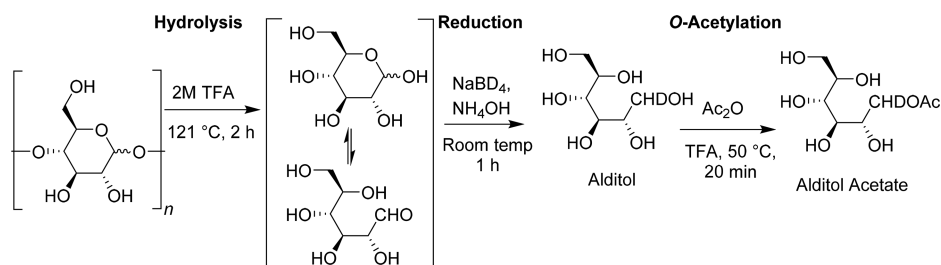


**Figure 2.** Selected portion of the HPLC-ELSD preparative separation chromatograms for fractions CJA2-03 and SNA-03 (Atlantis dC<sub>18</sub>). Compounds **1** and **2** were both obtained from the respective Fr.4 (~23–24 min) and Fr.5 (~24–25 min) fractions of both parent materials (arrows). This chromatogram shows the relative resolution and initial elution profiles for these fractions. See Figures S11 and S12 (Supporting Information) for representative ELSD and UV chromatograms for these separations.



**Scheme 1.** Alditol Acetate Derivatization of an Example Glucopyranosyl Unit for **1** or **2**



C

Supporting Information). Fractions SNA-03 and CJA2-03 each yielded two subfractions (Fr.4 and Fr.5 from each) that contained similar profiles of components by <sup>1</sup>H NMR and HPLC-ELSD profiling (Figures S10–S13, Supporting Information). Both Fr.4 subfractions, from both SNA-03 and CJA2-03, contained **1**, while both Fr.5 subfractions from the two parent materials contained **2** (Figure 2).

Fractions SNA-03 and -04 and CJA2-03, -04, and -05 contained the primary oligosaccharide profile of interest (Figures S5 and S6, Supporting Information) and, combined, accounted for 15% and 29% of SN and CJ starting materials, respectively. Although the SN fruit powder contained a lower overall percentage of oligosaccharide content, fraction SNA-03 constitutes a larger portion of the parent aqueous extract (44.3%) as compared to the parallel fraction CJA2-03 (22.6%). This is likely attributable to the fact that ~50% of the dry weight of the original SN material was removed as pectins or insoluble material through EtOH precipitation and subsequent filtration. Fractions SNA-03 and CJA2-03 were used for further purification steps, yielding compounds **1** and **2**, which composed ~0.13% and 0.29% w/w of SN and ~0.33% and 0.52% w/w of CJ, respectively. The combination of selected subfractions from the two parent materials provided sufficient material for full structure elucidation.

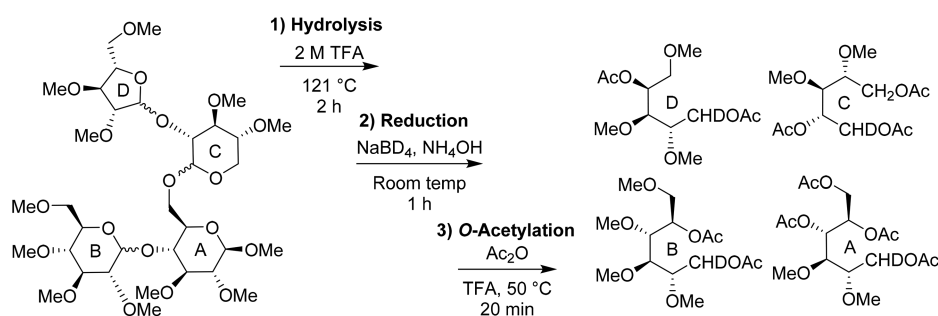
**MS Analysis.** The presence of neutral glycosyl residues in both **1** and **2** was indicated by initial <sup>1</sup>H NMR spectroscopic data and was confirmed using trimethylsilyl derivatization and GC-MS analysis (data not shown). Consequently, ionization using MS/TOF (data not shown) of both compounds in native form was minimal, requiring permethylation of free hydroxy groups to improve the intensity of indicative mass peaks.<sup>24</sup> Per-*O*-methylated **1** and **2** dissolved in 1 mM NaOH (50% MeOH(aq)) were analyzed by UHPLC/QTOFMS and yielded a high abundance of [M + NH<sub>4</sub>]<sup>+</sup> molecular ions, consistent with patterns observed in analyses of olive pulp and other oligosaccharides.<sup>25,26</sup> Per-*O*-methylated **1** eluted at 4.9 and 5.1 min and yielded [M + NH<sub>4</sub>]<sup>+</sup> and [M + Na]<sup>+</sup> molecular ions (*m/z* 1360.6652 and 1365.6263, respectively), with [M + NH<sub>4</sub>]<sup>+</sup> at 100% relative intensity in both eluted peaks (Figure S14, Supporting Information). Per-*O*-methylated **2** eluted at 5.2 and 5.4 min and yielded the same types of molecular ions as per-*O*-methylated **1** at *m/z* 1520.7398 and 1525.6988, respectively (Figure S14, Supporting Information). The observation of two elution peaks is consistent with the presence of  $\alpha$ - and  $\beta$ -anomers of the methyl glycoside derivative of the reducing glycosyl unit present in each native compound. Ions were also detected at *m/z* 689.3450 and 769.3771, corresponding to doubly charged molecular ions [M + 2NH<sub>4</sub>]<sup>2+</sup> as observed for xylan-type oligosaccharides.<sup>25</sup> Fragmentation patterns resulting from tandem-MS analyses can aid in determining the order of glycosyl units; however

Table 1. Results from the Chemical Derivatization Analyses for Compounds 1 and 2

glycosyl unit	alditol acetate analysis			D/L configuration		glycosyl linkage analysis		
	glycosyl identity	RT <sup>a</sup> (min)	molar ratio	glycosyl stereoisomer	RT (min)	ring size and linkage position	distinguishing mass fragments (m/z)	RRT <sup>b</sup>
Compound 1								
A	glucose	26.88	4	D-(+)-glucose	18.02	4,6-linked glcp	118, 261	0.776
B						4-linked glcp	118, 233	0.654
C						4,6-linked glcp	118, 261	0.776
D						terminal glcp	118, 161, 162, 205	0.497
E	xylose	21.73	2	D-(+)-xylose	18.76	2-linked xylp	117, 190	0.569
F						terminal xylp	117, 118, 161, 162	0.438
G	arabinose	19.82	1	L-(+)-arabinose	18.62	terminal araf	118, 161, 162	0.394
Compound 2								
A	glucose	27.06	2	D-(+)-glucose	18.02	4,6-linked glcp	118, 261	0.776
B						4-linked glcp	118, 233	0.655
C						4,6-linked glcp	118, 261	0.776
D						terminal glcp	118, 161, 162, 205	0.497
E	xylose	21.8	1	D-(+)-xylose	18.76	2-linked xylp	117, 190	0.569
F						2-linked xylp	117, 190	0.569
G	arabinose	19.9	1	L-(+)-arabinose	18.62	terminal araf	118, 161, 162	0.394
H						terminal araf	118, 161, 163	0.394

<sup>a</sup>RT, retention time. <sup>b</sup>RRT, relative retention time, RT of sample relative to the internal standard *myo*-inositol.

Scheme 2. Partially Methylated Alditol Acetate Derivatization Involving a Partial Structure of 2



minimal fragmentation was observed in the QTOFMS spectra for the permethylated derivatives of **1** and **2**. This is consistent with the branching pattern, as the level of fragmentation is negatively correlated with the level of branching in carbohydrates.<sup>27</sup> The molecular formulas, degrees of polymerization (DP), and numbers of pentose and hexose sugar residues were calculated from the exact masses: **1** (C<sub>39</sub>H<sub>66</sub>O<sub>33</sub>), DP = 7 with four hexose and three pentose moieties, and **2** (C<sub>44</sub>H<sub>74</sub>O<sub>37</sub>), DP = 8 with four hexose and four pentose moieties.

**Alditol Acetate Analysis.** As both **1** and **2** were neutral molecules, alditol acetate (AA) derivatization was appropriate for the identification of individual glycosyl units and subsequent molar ratio calculations. AA derivatives of **1** and **2**, generated through successive hydrolysis, reduction with NaBD<sub>4</sub>, and O-acetylation,<sup>28</sup> yielded indicative fragment pairs of deuterated pentose (*m/z* 290/291) and hexose (*m/z* 361/362) AA derivatives. This process is shown for an example glucopyranosyl unit in Scheme 1. The presence of glucose, arabinose, and xylose was confirmed based on comparisons of retention times and MS data to standards (Table 1; Figure S15 and Table S3, Supporting Information). Molar ratios, calculated based on quantification of AA derivatives of the monomers within each oligosaccharide, were applied to the DP to establish the presence of one arabinosyl, two xylosyl, and four glucosyl moieties in **1** and two arabinosyl, two xylosyl, and

four glucosyl moieties in **2**. This result is consistent with the numbers of pentosyl and hexosyl moieties calculated based on the observed mass of each compound.

**D/L Configuration.** The absolute configurations of the constituent monosaccharide moieties of **1** and **2** were determined using the parent fraction SNA-03 in order to preserve purified compounds. The sample and standards were hydrolyzed and treated with L-cysteine methyl ester and phenyl isothiocyanate to form optically active phenyl thiocarbamate (PTC) diastereomers, which were analyzed by HPLC-UV.<sup>29</sup> Comparisons of the retention times of standards to those of the PTC derivatives of SNA-03 (Table 1; Table S4, Figures S16–S19, and Section S4d, Supporting Information) indicated the presence of D-(+)-glucose, L-(+)-arabinose, and D-(+)-xylose, thus confirming the absolute configurations of the monomeric constituent units of **1** and **2**.

**Glycosyl Linkage Analysis.** Derivatives obtained through per-O-methylation followed by AA derivatization identified the ring size and linkage position of each monomeric unit upon GC-MS analysis (Scheme 2). Key patterns of O-methyl and O-acetyl substitutions resulted in distinguishing mass fragments for the partially methylated alditol acetate (PMAA) derivatives of **1** and **2** (Table 1). Relative retention times and mass fragments were compared to standards to characterize the carbohydrate monomers in each compound (Table S5 and Figure S20, Supporting Information). Compound **2** differed

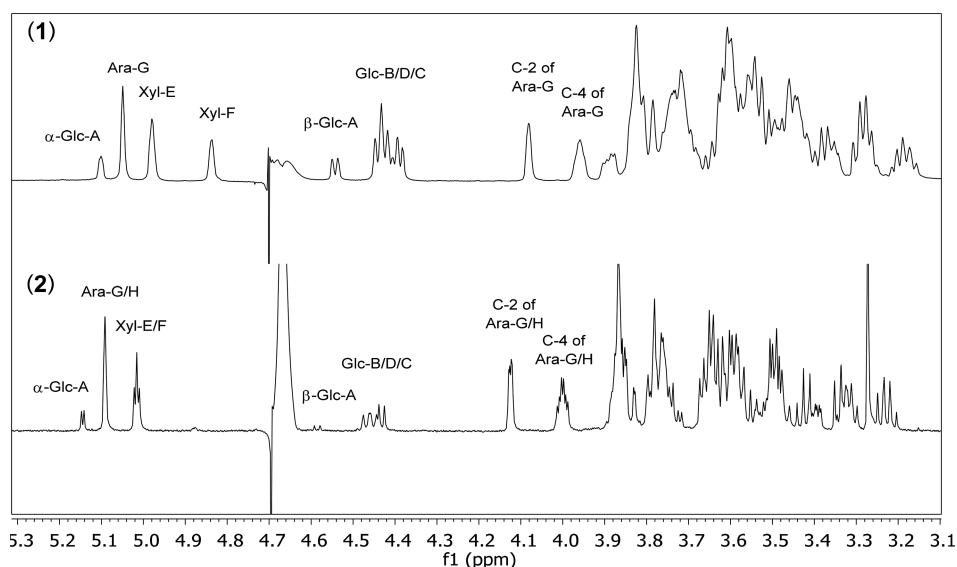


**Figure 3.**  $^1\text{H}$  NMR spectra for compounds **1** and **2**, with anomeric and selected protons indicated ( $\text{D}_2\text{O}$ , 600 MHz). See Figures S21–S23 (Supporting Information) for full spectra and expansions.

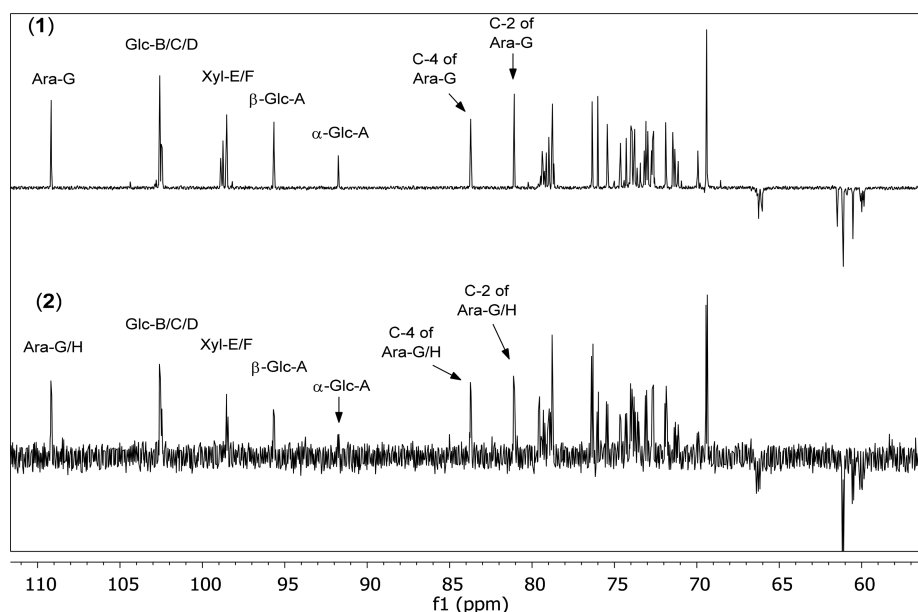


**Figure 4.**  $^{13}\text{C}$  DEPT NMR spectra for compounds **1** and **2**, with anomeric and selected carbons indicated ( $\text{D}_2\text{O}$ , 150 MHz). See Figures S24–28 (Supporting Information) for  $^{13}\text{C}$  NMR spectra and DEPT full spectra and expansions.

from **1** in the presence of a second terminal arabinofuranosyl moiety and replacement of the terminal xylopyranosyl unit with a 2-linked xylopyranosyl moiety.

**NMR Data Analysis.** The NMR-based structural elucidation of each compound was initiated independently. Later comparisons between the 1D and 2D NMR spectra and partial structures for both compounds helped to assign chemical shift values for the glycosyl backbones (Figures 5 and 6, Table 2). The  $^1\text{H}$  NMR spectrum of **1** (Figure 3; Figures S21–S23, Supporting Information) contained eight proton resonances in the anomeric region ( $\delta_{\text{H}}$  4.3–5.1) that integrated to a total of seven protons, thus indicating the presence of one reducing glycosyl unit (Glc-A, Figure 5). The anomeric protons gave HSQC correlations to eight carbon resonances in the  $\delta_{\text{C}}$  90–110 region (Table 2, Figure 7; Figures S27–S29, Supporting

Information), including two correlations pertaining to the  $\alpha$ - and  $\beta$ -anomers of the reducing Glc-A moiety.

The anomeric orientation of each glycosyl unit in **1** was determined through examination of chemical shift and coupling constant values for anomeric protons compared to reference spectra (Table 2, Figure 3; Figure S8, Supporting Information).<sup>30–32</sup> H-1 and H-2 of Ara-G ( $\delta_{\text{H}}$  5.04 and 4.07, respectively) gave  $^3J_{1,2} = 1.9$  Hz, indicating an  $\alpha$ -orientation for H-1, in agreement with published  $^3J_{1,2}$  values for  $\alpha$ -L-arabinofuranosides.<sup>31,32</sup>

The  $^4\text{C}_1$  preferred conformations of the xylopyranose and glucopyranose residues are similar, resulting in  $\alpha$ -anomeric protons with deshielded (e.g.,  $\delta_{\text{H}} > 4.70$ ) chemical shifts and coupling constants of  $^3J_{1,2} < 5$  Hz, while those with  $\beta$ -anomeric protons exhibit shielded (e.g.,  $\delta_{\text{H}} < 4.70$ ) chemical shifts and coupling constants of  $J_{1,2} > 5$  Hz. Accordingly, both xylosyl

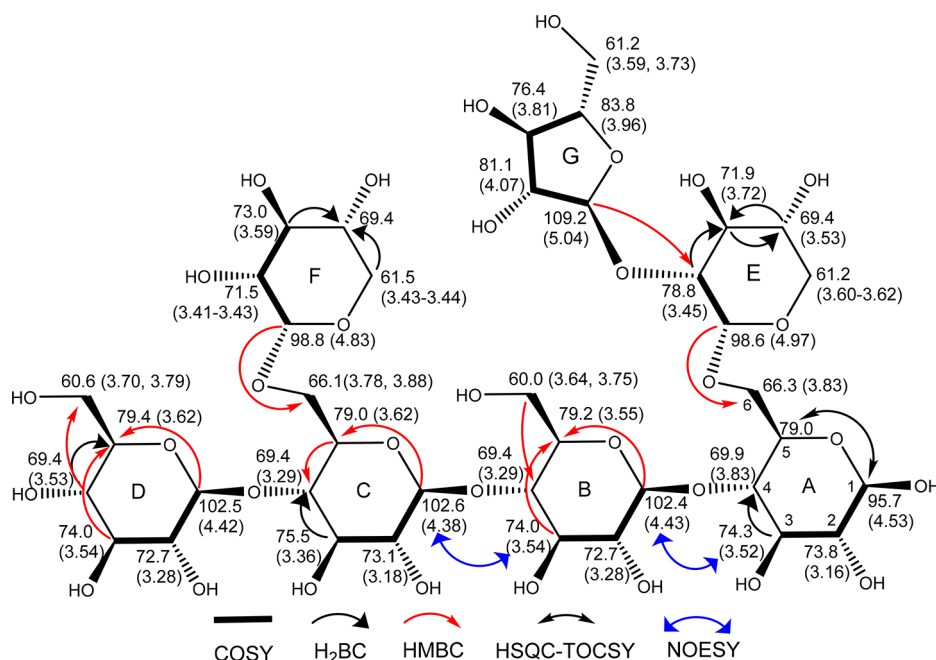


**Figure 5.** Key COSY, H2BC, HMBC, HSQC-TOCSY, and NOESY correlations for compound 1 with  $^{13}\text{C}$  and  $^1\text{H}$  chemical shifts indicated at each position [ $\delta_{\text{C}}$  ( $\delta_{\text{H}}$ )].

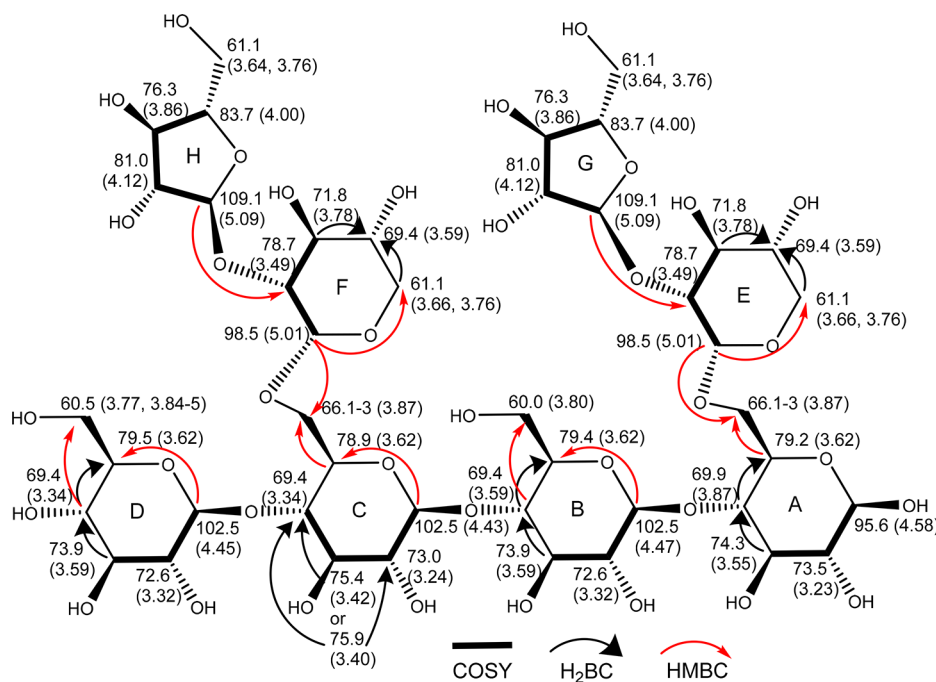


**Figure 6.** Key COSY, H2BC, and HMBC correlations for compound 2 with  $^{13}\text{C}$  and  $^1\text{H}$  chemical shifts indicated at each position [ $\delta_{\text{C}}$  ( $\delta_{\text{H}}$ )].

residues ( $\delta_{\text{H}}$  4.97 and 4.83) were  $\alpha$ -anomers, with  $^3J_{1,2} = 2.74$  and 3.32 Hz, respectively, while Glc-B, Glc-C, and Glc-D ( $\delta_{\text{H}} = 4.43, 4.38,$  and  $4.42,$  respectively) were  $\beta$ -anomers with  $^3J_{1,2} = 7.6, 7.1,$  and  $7.1$  Hz, respectively. The reducing nature of Glc-A resulted in duplicate resonances for the anomeric proton ( $\delta_{\text{H}} = 5.09$  and  $4.53$ ) and carbon ( $\delta_{\text{C}} = 91.8$  and  $95.7,$  respectively) corresponding to both the  $\alpha$ - and  $\beta$ -anomers ( $^3J_{1,2} = 3.6$  and  $7.6$  Hz, respectively) (Table 2).

The remaining proton and carbon resonances (Figures 3 and 4; Figures S21–26, Supporting Information) were assigned using the HSQC spectrum (Figure S29, Supporting

Information) in combination with additional 2D NMR experiments (Figures S30–S37, Supporting Information). Several methine carbons resonating in the  $\delta_{\text{C}}$  69.0–85.0 region were assigned using COSY, H2BC, and HMBC correlations. The congestion of resonances in the  $\delta_{\text{H}}$  3.10–3.85 region required the use of HSQC-TOCSY and phase-sensitive COSY experiments to assign C-5 and C-6 of Glc-A and C-6 of Glc-C (Figure 5; Figures S35 and S37, Supporting Information). The HSQC-TOCSY experiment established the assignment of the resonance at  $\delta_{\text{C}}$  79.0 to C-5 of Glc-A, but a corresponding H-5 resonance could not be identified due to a

Table 2.  $^1\text{H}$  and  $^{13}\text{C}$  NMR Assignments for Compounds 1 and 2 ( $\text{D}_2\text{O}$ , 600/150 MHz)

	compound 1			compound 2			compound 1			compound 2	
	C	$\delta^{13}\text{C}$	$\delta^1\text{H}$ (J in Hz <sup>a</sup> )	$\delta^{13}\text{C}$	$\delta^1\text{H}$ (J in Hz)		C	$\delta^{13}\text{C}$	$\delta^1\text{H}$ (J in Hz)	$\delta^{13}\text{C}$	$\delta^1\text{H}$ (J in Hz)
Glc-p-A	1	95.7	4.53 d (7.6)	95.6	4.58 d (8.0)	Glc-p-D	1	102.5	4.42 d (7.1)	102.5	4.45 d (8.0)
$\beta$ -anomer	2	73.8	3.16 t (9.4)	73.5	3.23		2	72.7	3.28 t (3.8)	72.6	3.32
	3	74.3	3.52	74.3	3.55		3	74.0	3.54	73.9	3.59
	4	69.9	3.83	69.9	3.87		4	69.4	3.53	69.4	3.34
	5	79.0		79.2	3.62		5	79.4	3.62	79.5	3.62
	6	66.3	3.83	66.1/66.3 <sup>b</sup>	3.87		6	60.6	3.70, 3.79	60.5	3.77, 3.84–5
Glc-p-A	1	91.8	5.09 d (3.6)	91.7	5.14 d (3.9)	Xyl-p-E	1	98.6	4.97 d (2.7)	98.5	5.01 d (3.8)
$\alpha$ -anomer	2	71.2	3.41–3.43	71.2	3.51		2	78.8	3.45	78.7	3.49
	3	73.2	3.71	73.5	3.23		3	71.9	3.72	71.8	3.78
	4	69.9	3.83	69.9	3.87		4	69.4	3.53	69.4	3.59
	5						5	61.2	3.60–3.62	61.1	3.66, 3.76
	6	66.3	3.83			Xyl-p-F	1	98.8	4.83 d (3.3)	98.5	5.01 d (3.8)
Glc-p-B	1	102.5	4.43 d (7.6)	102.5	4.47 d (8.2)		2	71.5	3.41–3.43	78.7	3.49
	2	72.7	3.28 t (8.8)	72.6	3.32		3	73.0	3.59	71.8	3.78
	3	74.0	3.54	73.9	3.59		4	69.4		69.4	3.59
	4	69.4	3.29 t (9.2)	69.4	3.59		5	61.5	3.43–3.44	61.1	3.66, 3.76
	5	79.2	3.55	79.4	3.62	Araf-p-G	1	109.2	5.04 br. d (1.9)	109.1	5.09 br. d (2.0)
	6	60.0	3.64, 3.75	59.8/60.0	3.80, 3.72, 3.87, 3.83		2	81.1	4.07	81.0	4.12 dd (3.8, 1.6)
							3	76.4	3.81	76.3	3.86
Glc-p-C	1	102.6	4.38 d (7.1)	102.5	4.43 d (7.8)		4	83.8	3.96 m	83.7	4.00 m
	2	73.1	3.18 t (7.9)	73.0	3.24		5	61.2	3.59, 3.73	61.1	3.64, 3.76
	3	75.5	3.36	75.4 <sup>c</sup>	3.42	Araf-p-H	1	NA		109.1	5.09 br. d (2.0)
				75.9 <sup>c</sup>	3.40		2	NA		81.0	4.12 dd (3.8, 1.6)
	4	69.4	3.29 t (9.2)	69.4	3.34		3	NA		76.3	3.86
	5	79.0	3.62	78.9	3.62		4	NA		83.7	4.00 m
	6	66.1	3.78, 3.88 dd (11.0, 5.0)	66.1/66.3 <sup>b</sup>	3.87 dd		5	NA		61.1	3.64, 3.76

<sup>a</sup>Only coupling constants that could be measured accurately are shown. <sup>b</sup>Two resonances for C-6 of Glc-A and C in 2 were present at 66.1 and 66.3; however, the two could not be distinguished with the present data, and both are assigned as 66.1/66.3. <sup>c</sup>Two carbon and proton chemical shift pairs could be assigned for C-3 of Glc-C.

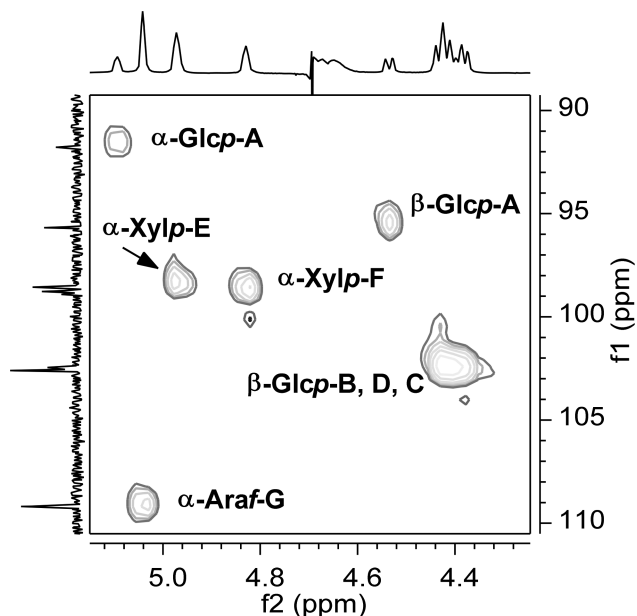


Figure 7. Expansion of the anomeric region of the HSQC spectrum for compound 1 with labeled correlations ( $\text{D}_2\text{O}$ , 600/150 MHz). See Figure S29 (Supporting Information) for full HSQC spectrum of compound 1.

lack of correlation. As the assignments of C-6 for Glc-A and Glc-C were integral for determining the locations of the Xyl-E-

Ara-G and Xyl-F side chains, a phase-sensitive COSY spectrum (Figure S37, Supporting Information) was used to differentiate between the two unassigned oxymethylene carbons at  $\delta_{\text{C}}$  66.1 and 66.3 in 1. The objective of this experiment was to detect a correlation with the well-resolved proton resonance observed at  $\delta_{\text{H}}$  3.88 (dd) associated with the carbon resonating at  $\delta_{\text{C}}$  66.1 via HSQC data. The observed correlation between the  $\delta_{\text{H}}$  3.88 proton resonance and H-5 ( $\delta_{\text{H}}$  3.62) of Glc-C unequivocally established the chemical shifts of C-6 and H-6 of Glc-C in 1 as  $\delta_{\text{C}}$  66.1 and  $\delta_{\text{H}}$  3.88, respectively, and, by elimination, C-6 of Glc-A at  $\delta_{\text{C}}$  66.3 in 1. The nature of the  $\beta$ -(1 $\rightarrow$ 4)-glucose backbone for 1 was established based on comparisons to spectra for celotetraose and compound 2 (Figures S38 and S39, Supporting Information) and the presence of indicative NMR correlations. The NOESY spectrum of 1 (Figure 5; Figure S36, Supporting Information) contained correlations between H-3 ( $\delta_{\text{H}}$  3.52) of Glc-A and H-1 ( $\delta_{\text{H}}$  4.43) of Glc-B and between H-3 ( $\delta_{\text{H}}$  3.54) of Glc-B and H-1 ( $\delta_{\text{H}}$  4.38) of Glc-C. The presence of a (1 $\rightarrow$ 2)-linkage between Ara-G and Xyl-E for 1 was indicated by an HMBC correlation (Figure 5; Figure S44, Supporting Information) between H-1 ( $\delta_{\text{H}}$  5.04) of Ara-G and C-2 ( $\delta_{\text{C}}$  78.8) of Xyl-E. The (1 $\rightarrow$ 6)-linkages between xylosyl and glucosyl residues were indicated by HMBC correlations between H-1 ( $\delta_{\text{H}}$  4.97) of Xyl-E and C-6 ( $\delta_{\text{C}}$  66.3) of Glc-A and between H-1 ( $\delta_{\text{H}}$  4.83) of Xyl-F and C-6 ( $\delta_{\text{C}}$  66.1) of Glc-C, thus locating the E $\rightarrow$ G- and F- glycosyl moieties on alternating glucosyl residues.

Based on NMR correlations and the derivatization results, the structure of **1** was defined as the heptasaccharide  $\beta$ -D-glucopyranosyl-(1 $\rightarrow$ 4)-[ $\alpha$ -D-xylopyranosyl-(1 $\rightarrow$ 6)]- $\beta$ -D-glucopyranosyl-(1 $\rightarrow$ 4)- $\beta$ -D-glucopyranosyl-(1 $\rightarrow$ 4)-[ $\alpha$ -L-arabinofuranosyl-(1 $\rightarrow$ 2)]- $\alpha$ -D-xylopyranosyl-(1 $\rightarrow$ 6)]- $\beta$ -D-glucopyranose.

The  $^1\text{H}$  NMR spectrum of **2** (Figure 3; Figures S21–S23, Supporting Information) contained seven resonances in the anomeric region that integrated to eight protons. The anomeric proton resonances at  $\delta_{\text{H}}$  5.01 ( $^3J_{1,2} = 3.8$  Hz, 2H) and 5.09 ( $^3J_{1,2} = 2.0$  Hz, 2H) were identified as those of  $\alpha$ -xylosyl and  $\alpha$ -arabinosyl residues, respectively, while the resonances at  $\delta_{\text{H}}$  5.14 ( $^3J_{1,2} = 3.9$  Hz) and 4.58 ( $^3J_{1,2} = 8.0$  Hz) corresponded to the respective  $\alpha$ - and  $\beta$ -anomers of a reducing glucosyl residue (Table 2 and Figure 6). The anomeric protons gave HSQC correlations to five carbon resonances in the  $\delta_{\text{C}}$  91–110 region (Table 2, Figure 4; Figures S22–S28 and S40, Supporting Information), with the two at  $\delta_{\text{H}}$  5.14 and 4.58 correlating with the  $\alpha$ - and  $\beta$ -anomers of Glc-A ( $\delta_{\text{C}}$  91.7 and 95.6, respectively), one ( $\delta_{\text{H}}$  5.01; 2H) correlating with the two xylosyl moieties ( $\delta_{\text{C}}$  98.5; 2C; Xyl-E and Xyl-F), and one ( $\delta_{\text{H}}$  5.09; 2H) correlating with the two arabinosyl moieties ( $\delta_{\text{C}}$  109.1; 2C; Ara-G and Ara-H). The three remaining anomeric protons ( $\delta_{\text{H}}$  4.47,  $^3J_{1,2} = 8.2$  Hz; 4.43,  $^3J_{1,2} = 7.8$  Hz; and 4.45,  $^3J_{1,2} = 8.0$  Hz) were consistent with nonreducing  $\beta$ -glucosyl residues ( $\delta_{\text{C}}$  102.5; 3C) and corresponded to the Glc-B, Glc-C, and Glc-D moieties. The remaining proton and carbon resonances were assigned using the HSQC spectrum in conjunction with COSY, H2BC, and HMBC data (Table 2, Figure 6; Figures S40–47, Supporting Information).

HMBC correlations (Figure 6; Figure S44, Supporting Information) between H-1 of the Ara moieties ( $\delta_{\text{H}}$  5.09) and C-2 of the Xyl moieties ( $\delta_{\text{C}}$  78.7) confirmed the presence of two arabinosyl-(1 $\rightarrow$ 2)-xylosyl linkages identical to those present in **1**. Correlations between H-1 of the Xyl moieties ( $\delta_{\text{H}}$  5.01) and C-6 of Glc-A and C ( $\delta_{\text{C}}$  66.1/66.3) also matched the branching pattern of **1**. While neither NOESY nor HMBC spectra provided specific correlations indicating the linkages between the glucosyl moieties due to overlap of the Glc-B, Glc-C, and Glc-D resonances, the same  $\beta$ -(1 $\rightarrow$ 4)-glucosyl backbone was assigned due to the similarities observed in the spectra of **1**, **2**, and cellotetraose (Figures S38 and S39, Supporting Information).

In contrast with **1**, compound **2** showed considerable conformational flexibility. This was indicated by more than two correlations between proton resonances and the C-6 oxy-methylene carbons of Glc-B ( $\delta_{\text{C}}$  60.0) and Glc-D ( $\delta_{\text{C}}$  60.5, Table 2). The  $\delta_{\text{C}}$  60.0 resonance of Glc-B is observed as two small signals at  $\delta_{\text{C}}$  59.85 and 60.0, which were considered together as a single resonance. C-3 of Glc-C ( $\delta_{\text{C}}$  75.4) also gave correlations indicative of conformational flexibility and labile hydrogen bonding. Hydrogen bonding between the tetrahydropyran heteroatom and the 3-hydroxy of an adjacent glucosyl moiety is a common feature of a cellulosic  $\beta$ -D-(1 $\rightarrow$ 4)-glucose backbone.<sup>33</sup> In the case of **2**, C and H resonances vicinal to C-3/H-3 of Glc-C showed dual correlations with two separate C-3/H-3 pairs ( $\delta_{\text{C}}$  75.4/ $\delta_{\text{H}}$  3.42 and 75.9/ $\delta_{\text{H}}$  3.40) in COSY, H2BC, and HMBC spectra (Figures S42–S44, Supporting Information). Resonances at  $\delta$  75.4 and 75.9 were therefore both assigned to C-3 of Glc-C.

Based on NMR correlations and the derivatization results, the structure of **2** was defined as the octasaccharide  $\beta$ -D-glucopyranosyl-(1 $\rightarrow$ 4)-[ $\alpha$ -L-arabinofuranosyl-(1 $\rightarrow$ 2)]- $\alpha$ -D-xylo-

pyranosyl-(1 $\rightarrow$ 6)]- $\beta$ -D-glucopyranosyl-(1 $\rightarrow$ 4)- $\beta$ -D-glucopyranosyl-(1 $\rightarrow$ 4)-[ $\alpha$ -L-arabinofuranosyl-(1 $\rightarrow$ 2)]- $\alpha$ -D-xylopyranosyl-(1 $\rightarrow$ 6)]- $\beta$ -D-glucopyranose.

### Comparisons of **1** and **2** to Known Xyloglucans.

Naturally occurring xyloglucans are a common type of hemicellulose present in the primary cell walls of higher plants.<sup>33,34</sup> The solubilization and enzymatic depolymerization of hemicellulosic polysaccharides such as xyloglucans is a feature of fruit ripening<sup>35</sup> and contributes to the physical softening of fruit.<sup>36</sup> Xyloglucans are composed of repeating units of a cellotetraose backbone containing  $\beta$ -D-(1 $\rightarrow$ 4)-glucopyranosyl residues with  $\alpha$ -D-(1 $\rightarrow$ 6)-xylopyranosyl substituents (side chains) attached to the glucosyl moieties. Xylopyranosyl moieties are often substituted with galactose or  $\alpha$ -L-(1 $\rightarrow$ 2)-arabinofuranosyl moieties,<sup>37</sup> increasing the solubility of these compounds when dissociated from cellulose. Arabinoxyloglucan polymers have been identified in tomato, potato, and tobacco (Solanaceae),<sup>37</sup> and similar parent polymers are likely to be the source of the oligosaccharides found in cranberry products. As compounds **1** and **2** were both identified in both source materials, it is possible that these compounds originate from the natural process of cranberry fruit ripening. A similar series of oligosaccharides has also been detected in cranberry concentrate material (Ocean Spray Cranberries, Inc., Lakeville-Middleboro, MA, USA) using methods similar to those presented here.<sup>38</sup> Further work will be necessary to determine the effects of various commercial processing and product preparation methods on cranberry oligosaccharide content and profiles in different products.

Compounds **1** and **2** are previously uncharacterized oligosaccharides that possess structural characteristics similar to those reported elsewhere for cranberry oligosaccharides.<sup>16,17,21,22</sup> The repeating oligosaccharide units identified from Solanaceous plants<sup>37</sup> differ from those of **1** and **2** in that the branch side chains of Solanaceous oligosaccharides are located on adjacent glucose moieties. This observation may be due, in part, to the methods used to generate the various oligomers from the parent polymers being studied. Other reports of cranberry xyloglucans provide MALDI-TOF/TOF MS/MS fragmentation pattern evidence for both adjacent and alternate placements of branch side chains.<sup>16,17</sup> PTC derivatives of the parent fraction SNA-03 yielded only four monomeric units, D-(+)-glucose, D-(+)-xylose, L-(+)-arabinose, and D-(+)-galactose, indicating that additional oligosaccharides may be present in the cranberry series that contain galactosyl moieties. From these data, it is likely that the overall cranberry oligosaccharide profile contains both types of branching motifs (alternate and adjacent), in conjunction with variations in side chain composition.

**Bioactivity. Antimicrobial and Cell Viability Assays.** All cranberry materials tested were ineffective at inhibiting the growth of the pathogenic microorganisms used in the NCNPR antimicrobial screening assay (Table S6, Supporting Information). Compounds **1** and **2** and oligosaccharide-enriched fractions also did not exhibit cytotoxic effects against two different breast cancer cell lines (Table S7, Supporting Information). These preliminary data suggest that the reported antiproliferative<sup>39,40</sup> and antimicrobial<sup>41,42</sup> effects of cranberry extracts are due to compounds other than arabinoxyloglucan oligosaccharides. In this case, the lack of activity for the tested compounds and fractions is considered to be a positive result, as it supports possible mechanisms of microbial disease prevention or treatment that involve noncytotoxic effects. If

compounds such as cranberry oligosaccharides were to be developed into products intended for the management or prevention of diseases such as UTIs, resistance development associated with long-term or repeated use would be less likely to cause problems.

**Antiadhesion Properties.** The EC-UEC antiadhesion assay used in this study was under development during the time period when samples were submitted. A series of unexpected methodological and sample-management issues (Section S2, [Supporting Information](#)) arose during testing, and the data reported herein are therefore considered to be preliminary. The relative activity of each test sample was based on qualitative assessments of the dose–response curves obtained at the sample concentrations tested relative to that of the positive control, myricetin (Figure S48, [Supporting Information](#)). Samples with an overall negative slope were considered active (e.g., Figure S49 C and D, [Supporting Information](#)), while samples with an overall positive slope were considered inactive (e.g., Figure S50 A, [Supporting Information](#)). Samples in which a negative slope appears at higher concentrations (e.g., Figure S50 B and C, [Supporting Information](#)) were considered potentially active, as these samples may have resulted in increased antiadhesion effects if tested at higher concentrations.

The aqueous SN extract (SNA) and subfractions SNA-03 and SNA-04 exhibited dose-dependent antiadhesive effects as determined by the observation that the slopes of the dose–response curves for these samples were negative, similar to that of myricetin. This effect appears to be greater with SNA, as this sample yielded a dose–response curve with an increased slope and lower final cpm values relative to myricetin and subfractions SNA-03 and SNA-04. The HPLC subfractions that contained compounds 1 and 2 (SNA-03 Fr.4, Fr.5, and Fr.6) and the purified compounds 1 (from SNA-03 Fr.4) and 2 (from SNA-03 Fr.5) showed a lack of antiadhesion activity relative to the parent material SNA-03 and the positive control (Figures S50 and S51, [Supporting Information](#)). Fractions SNA-03 Fr.5, Fr.6, and Fr.9 (Figure S50 B, C and Figure S52 E, [Supporting Information](#)) resulted in dose–response curves that displayed negative slopes above the test concentration of 7 mg/mL, suggesting that higher test concentrations may have resulted in greater antiadhesion properties. The remaining SNA-03 fractions, Fr.1, Fr.3, Fr.7, and Fr.8, showed a lack of antiadhesion activity (Figure S52, [Supporting Information](#)).

The higher antiadhesion activity of the parent fraction SNA relative to that of the Sephadex LH-20 fraction SNA-03 and the subsequent RP-HPLC fractions of SNA-03 (e.g., Fr.4, Fr.5) supports the theory that multiple compounds as mixtures may exhibit greater antiadhesion activity than fractions or purified components. Further studies on Sephadex LH-20 fractions containing only oligosaccharide components obtained from cranberry juice concentrate<sup>38</sup> provide additional evidence that mixtures of cranberry oligosaccharides prevent the adhesion of uropathogenic *E. coli* adhesion to uroepithelial cells. The relative contributions of individual cranberry oligosaccharide components to overall antiadhesion activity, however, will require further studies such as those that use proportional recombinations of fractions or purified compounds to identify additive or synergistic effects. Studies of this type and further investigations of concentration effects were beyond the scope of the present project due to limitations in both material and available resources.

An apparent loss of bioactivity as fractionation proceeds is a well-known phenomenon in the field of natural products research, and multiple possible reasons for this occurrence could be proposed. As several independent lines of evidence support the hypothesis that oligosaccharides are involved in the *in vivo* antiadhesive properties of cranberry materials,<sup>9,14–17,38</sup> it is proposed that such antiadhesion effects are possibly the result of (1) mixtures of various oligosaccharides within the series, (2) mixtures of oligosaccharides with other classes of compounds, (3) higher overall concentrations of oligosaccharides than could be tested in the present study, or (4) some combination of possibilities 1–3. The inherent *in vitro* nature of the bioassay further confounds the issue, as (1) various *in vivo* processes may contribute to the urinary antiadhesive effects of cranberry materials and (2) the antiadherence assay used may not be effective at detecting the mechanism by which cranberry oligosaccharides prevent *E. coli* adhesion. For further discussion see Section S3 ([Supporting Information](#)).

**Significance of Structural Features for Future Studies.** This is the first report describing the complete structure elucidation of two arabinoxyloglucan oligosaccharides from cranberry products. The new compounds 1 and 2 are representative of a series of structurally related oligosaccharides that possess chemical features that make these compounds difficult to detect and characterize without the application of specialized methods and techniques. These compounds are neutral carbohydrates that do not readily ionize or produce diagnostic fragments using standard MS-based detection methods. They are UV-transparent and require specialized detection via evaporative light scattering or refractive index detectors. They are of relatively high molecular mass (>500 Da) and are highly polar, requiring that relatively large mass quantities (>5 mg) of samples be solubilized in water or DMSO for spectroscopic analyses and that samples be dried via lyophilization. While methods are available for the complete structural analysis of these compounds, such methods are destructive, requiring fairly large quantities of purified starting material for multiple sample derivatizations and analyses. Some specialized resources are available for studying xyloglucans such as those found in cranberry materials, including NMR reference spectra and MS fragmentation data,<sup>30,37,43</sup> but the general applicability of such resources is confounded by the structural complexities inherent to carbohydrates.<sup>44</sup>

These compounds are difficult to isolate due to their polar nature and the close structural similarities of the compounds in the series. The use of Sephadex LH-20 as an initial enrichment method was a serendipitous discovery,<sup>14</sup> and subsequent attempts by our research group to use carbohydrate-specific isolation and purification methods, such as carbohydrate extraction resins, diol chromatography, hydrophilic-interaction chromatography, and various other sorbents and separation techniques, met with limited success. This is possibly due to the fact that the methods attempted are typically used for the isolation of carbohydrate monomers, dimers, or trimers, and therefore do not readily enrich for or resolve neutral oligosaccharides with DP > 6. Carbohydrates are often considered to be “nuisance compounds” in terms of natural products isolation. Methods and sorbents pertaining to carbohydrates are often intended to remove carbohydrates from a sample rather than to intentionally enrich for specific types of carbohydrates. The optimization of isolation or

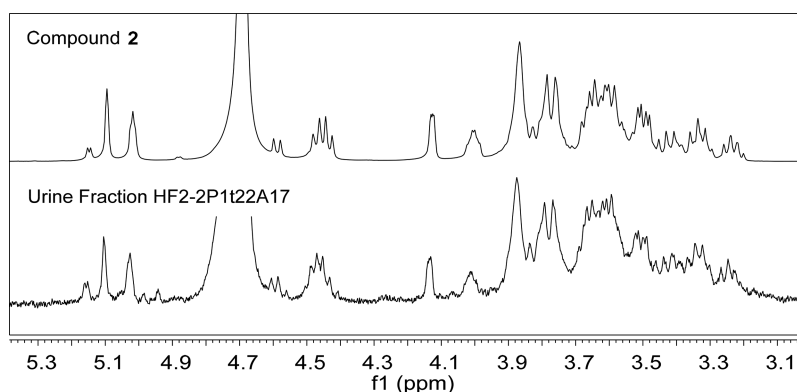


**Figure 8.** Comparison of the  $^1\text{H}$  NMR spectra for **2** (11.2 mg) and HF2-2P1t22A17 ( $\sim 2$  mg), an enriched fraction from porcine urine, showing similar composition ( $\text{D}_2\text{O}$ , 400 MHz). The HF2-2P1t22A17 material was obtained from a fraction of porcine urine that exhibited antiadhesive properties.<sup>15</sup> NMR and analytical HPLC-ELSD data for HF2-2P1t22A17 indicate that it contains a single primary component that is structurally related to an octasaccharide isolated from a related fraction. See the accompanying article<sup>15</sup> for a detailed discussion of the oligosaccharide series detected in porcine urine after cranberry consumption.

detection methods is made additionally difficult by the fact that applicable standards for this class of compound are not readily available. Knowledge of the complete structures of at least two compounds from the cranberry oligosaccharide series may aid future studies seeking to develop improved enrichment and isolation methods.

While the structural features of cranberry oligosaccharides make them difficult to detect, isolate, and chemically characterize, these same features may contribute to specific biological properties for these compounds. Several structural features support the hypothesis that these compounds could be directly absorbed and excreted into mammalian urine. High-MW, neutral oligosaccharides from other sources, such as human milk,<sup>45,46</sup> with as many as eight glycosyl units, have been detected in the urine of human infants, and cranberry oligosaccharides fall within this molecular size range.<sup>16</sup> The presence of Ara-Xyl-, Xyl-, and other types of glycosyl side chains<sup>16</sup> may contribute to the aqueous solubility of this class of compounds, as has been observed for other plant-derived polymeric xyloglucans<sup>37</sup> and by molecular dynamics simulations investigating xyloglucan intramolecular hydrogen bonding and solvation.<sup>47,48</sup> The possibility of direct absorption for cranberry oligosaccharides early in the digestive process is supported by the acid stability of the cellulose-type,  $\beta$ -(1 $\rightarrow$ 4)-glucose backbone<sup>49,50</sup> and by the detection of compounds with similar elution profiles and structural features in porcine urine (Figure 8) as discussed in the accompanying manuscript.<sup>15</sup> The conformational flexibility observed by NMR for compounds **1** and **2** in aqueous solution, combined with intra- and intermolecular hydrogen bonding, may contribute to the observed formation of microaggregates in solution.<sup>9</sup> The formation of such microaggregates may influence both the absorption and excretion of these compounds and their antiadhesion and other biological properties.

Structural characteristics of cranberry oligosaccharides, such as the presence of terminal arabinosyl residues and characteristic branching patterns, may influence the effects these compounds have on fecal microbes and thereby contribute to the gut health benefits of cranberry materials.<sup>23</sup> Specific strains of *Bifidobacterium longum* have been identified that can ferment cranberry xyloglucans similar to those described in this report at low rates, while other strains and organisms are not capable of using these compounds as a carbon source.<sup>22</sup>

Bacterial fermentation of cranberry xyloglucans involved the hydrolysis of a terminal arabinosyl moiety from the reducing end of the molecule (e.g., Ara-G for **1** and **2**). The ability of certain strains of beneficial bacteria to utilize specific substrates is known to impact the overall composition of the gut microbiota by multiple mechanisms.<sup>51</sup>

The gut is the primary reservoir for strains of *E. coli* that cause community acquired UTIs.<sup>52</sup> Cranberry compounds, including oligosaccharides with particular structural features, may help decrease the population of this pathogen in the gut reservoir by influencing the binding of certain strains of *E. coli* to mammalian epithelial cells and by providing a preferred, plant-cell-wall-based substrate for bacteria, enabling fecal clearance. Cranberry xyloglucan mixtures have been able to inhibit the in vitro adhesion of several different strains of *E. coli* to different types of epithelial cell lines.<sup>16</sup> The investigated strains of *E. coli* expressed various adhesins, including type 1, type IV, P-fimbriae, and the *E. coli* common pilus, and were affected differently by fractions of cranberry materials that contained various profiles of oligosaccharides and other compounds. A study investigating the adhesion of two enteropathogenic *E. coli* strains (O157:H7 and O18:K1:H7) to spinach leaves found that the *E. coli* common pilus allows these organisms to adhere to plant cells by targeting arabinosyl residues of pectin and other plant cell wall components.<sup>53</sup> This study used oligosaccharides with known structures and found that various structural features, such as backbone and side chain lengths, monosaccharide composition, branching patterns, and overall DP, influenced *E. coli* binding and adhesion processes. These types of specific oligosaccharide structural features, in combination with the type of *E. coli* adhesin being expressed, may therefore be of relevance for the various biological properties of cranberry oligosaccharides, especially with regard to the prevention of *E. coli* adhesion.

In conclusion, the series of structurally related oligosaccharides represented by compounds **1** and **2** is likely to play important roles in the bioactivities and health benefits attributed to the American cranberry (*V. macrocarpon*). Enriched oligosaccharide fractions and purified compounds exhibited a lack of antimicrobial and cytotoxic effects, supporting the potential use of such compounds for the prevention of disease without the risk for resistance development. Preliminary results from the antiadhesion assay used in

this study indicated that mixtures of oligosaccharides exhibited greater antiadhesion properties than more purified fractions or pure compounds. The potential use of cranberry oligosaccharides for the prevention of infection, especially UTIs, warrants continued investigation into the structural characteristics of this complex series of compounds.

## ■ EXPERIMENTAL SECTION

**General Experimental Procedures. Solvents and Chemicals.** Solvents were purchased from Fisher Chemicals (Thermo-Fisher Scientific, Waltham, MA, USA) and were ACS certified or HPLC-grade as appropriate unless otherwise stated. DMSO and MeOH were dried with 3 Å molecular sieves. Chemical reagents included Tri-Sil reagent (from Thermo-Fisher Scientific) and L-cysteine methyl ester and phenyl isothiocyanate (from Sigma-Aldrich, Inc., St. Louis, MO, USA). All carbohydrate standards and *myo*-inositol were purchased from Sigma-Aldrich unless otherwise stated. Cellotetraose was purchased from Dextra (Reading, UK), and Sephadex LH-20 (Lipophilic Sephadex LH-20, 25–100 µm bead size) was from Sigma-Aldrich. High-purity NMR solvents DMSO-*d*<sub>6</sub> (99.99%) and D<sub>2</sub>O (99.99%) were obtained from Cambridge Isotope Laboratories, Inc. (Andover, MA, USA).

**Equipment.** Analytical HPLC separations were performed using a Waters 2695 separations module equipped with an autosampler and a Waters 996 photodiode array (PDA) detector (Waters Corporation, Milford, MA, USA) and connected in series to a Polymer Laboratories PL-ELS 2100 evaporative light scattering detector (ELSD). Preparative HPLC separations were performed using a Waters Delta Prep 4000 HPLC equipped with a Waters 2487 dual wavelength absorbance detector connected in series to a Polymer Laboratories PL-ELS 1000 ELSD with a flow splitter for collection of eluent. UHPLC-MS/MS analyses were performed using an Agilent LC-1200 Infinity Series (1290) UHPLC system coupled to a QTOFMS (model #G6530A, Agilent Technologies, Palo Alto, CA, USA) with data acquisition and analysis controlled by Agilent MassHunter Acquisition software Ver. A.02.00 and processed by MassHunter Qualitative Analysis software Ver. B.02.00. GC-MS was performed using an Agilent Packard 6890 Series GC system coupled with a Hewlett-Packard 5973 mass selective detector, and data acquisition and analyses were performed using Agilent ChemStation and MestreNova software (Mestrelab Research, Escondido, CA, USA). NMR spectra were recorded on Bruker Avance III 400 MHz spectrometers equipped with 3 mm probes and either Ultrashield or Ultrashield Plus magnets. Additional NMR spectra for compounds **1** and **2** were obtained on a Bruker Avance II 600 MHz spectrometer (Bruker Biospin, Reinsetten, Germany).

**Isolation.** Two starting materials were used in this investigation: Sundown Naturals brand cranberry fruit powder (100 × 475 mg capsules; SN) (Rexall Sundown Inc., Boca Raton, FL, USA) and spray-dried cranberry hull extract powder (CJ), provided by Ocean Spray Cranberries, Inc. (Lakeville-Middleboro, MA, USA). Color images of these materials and their labeling are included in the [Supporting Information](#) (Figure S1). The CJ material was created by spray-drying cranberry juice (cranberry hull extract) that had been produced via proprietary methods. The CJ powder was fully soluble in water and produced a dark burgundy solution that was similar in appearance to commercially available cranberry juice products prepared from cranberry juice concentrate. The SN material appeared to be composed of ground, lyophilized cranberries mixed with powdered silica, as determined by available label information, product appearance, and behavior in solution.

The isolation methodology was based on methods developed and used to isolate oligosaccharides from porcine urine produced after the feeding of CJ cranberry powder.<sup>14,15</sup> The SN and CJ powders (40.0 g each) were dissolved separately in H<sub>2</sub>O (150 mL) and centrifuged for 5 min at 1800 rpm, and the precipitate was washed with H<sub>2</sub>O (1 × 100 mL and 1 × 50 mL) to yield water-soluble supernatants (300 mL each). The supernatants were extracted with EtOAc (4 × 150 mL), and aqueous fractions were concentrated by evaporation under

reduced pressure with a water bath temperature of ~40 °C. The SN aqueous fraction (250 mL) was further treated with EtOH (500 mL) to precipitate proteins and pectins using sonication (20 min) and centrifugation at 3000 rpm for 5 min. The resulting fractions were concentrated and dried via lyophilization to give EtOAc fractions SNE (0.31 g) and CJE (0.41 g) and aqueous SNA (14.04 g) and CJA (38.4 g).

SNA and CJA (13.7 and 25.3 g, respectively) were individually fractionated using Sephadex LH-20 (356 g dry resin, 7 × 37 cm column) equilibrated in 70% EtOH. Each sample was dissolved in 70% EtOH and centrifuged for 5 min at 2000 rpm to remove precipitate, yielding final load volumes of 60 and 100 mL for SNA and CJA, respectively. Both samples were fractionated using gravity-driven isocratic elution with 70% EtOH, flow rates of 1–2 mL/min, and the collection of 15–20 mL fractions. A time-lapsed color image of the fractionation of CJA material on Sephadex LH-20 (separation CJA1)<sup>15</sup> is included in the [Supporting Information](#) (Figure S2). Fractions were combined based on visual assessment and elution volume to yield five major fractions from each starting material: SNA-02 (1.14 g), SNA-03 (3.62 g), SNA-04 (2.44 g), SNA-05 (2.11 g), SNA-06 (3.06 g) and CJA2-02 (2.09 g), CJA2-03 (3.98 g), CJA2-04 (1.74 g), CJA2-05 (1.81 g), and CJA2-06 (3.81 g). Oligosaccharide-containing fractions of interest were identified using analytical HPLC-PDA-ELSD (Figures S3–S6, Table S1, and Section S4, [Supporting Information](#)). For the SNA column, fractions containing oligosaccharides, SNA-03 and SNA-04, eluted between 320 and 620 min and were dried to yield lavender-maroon powders. For the CJA2 column, fractions containing oligosaccharides, CJA2-03, CJA2-04, and CJA2-05, eluted between 350 and 810 min and were dried to yield pink-lavender powders. Material eluting before 320 and 350 min from the SNA and CJA2 columns, respectively, yielded fractions SNA-02 and CJA2-02.

Fractions CJA2-03 (1.0 g) and SNA-03 (3.17 g) were dissolved in H<sub>2</sub>O (4 and 9 mL, respectively), filtered (0.20 µm), and fractionated by RP-HPLC using a Waters Atlantis dC<sub>18</sub> (19 × 250 mm, 10 µm) column. Injection volumes ranged from 400 to 600 µL, and fractions were eluted using a gradient mobile phase of H<sub>2</sub>O to 30% MeOH over 30 min at a flow rate of 25 mL/min. Analytes were detected using a dual-wavelength UV detector (210 and 254 nm) connected in series to an ELSD. A flow splitter in line between the UV detector and the ELSD allowed for an ELSD inlet solvent flow rate of 1–2 mL/min and parallel collection of the remaining eluent. The ELSD used N<sub>2</sub> as the carrier gas at a flow rate of 0.8 SLM, a nebulizer temperature of 50 °C, and an evaporator temperature of 100 °C. Multiple fractions were collected and combined based on retention times and similar retention profiles (Table S2, Figures S11 and S12, [Supporting Information](#)). For the SNA-03 fractionation, analytes eluting at 23.8–24.5 and 24.5–25.5 min were collected and pooled to yield fractions SNA-03 Fr.4 (149 mg) and SNA-03 Fr.5 (212 mg), respectively (Figure 2). For the CJA2-03 fractionation, analytes eluting between 23.4–24.3 and 24.3–25.3 min were pooled to yield CJA2-03 Fr.4 (56 mg) and CJA2-03 Fr.5 (97 mg), respectively (Figure 2). These selected subfractions (SNA-03 Fr.4, SNA-03 Fr.5, CJA2-03 Fr.4, and CJA2-03 Fr.5) were analyzed by <sup>1</sup>H NMR spectroscopy (Figure S10, [Supporting Information](#)) and chosen for further purification.

SNA-03 Fr.4 (80.1 mg), SNA-03 Fr.5 (169.4 mg), and CJA2-03 Fr.5 (60 mg) were fractionated by NP-HPLC using a YMC Polyamine II column (20 × 250 mm, 5 µm) and an isocratic mobile phase of 63% MeCN(aq). Samples were dissolved in sufficient volumes of 50% MeOH(aq) to give concentrations of 0.1 mg/mL, and injection volumes ranged from 100 to 200 µL per run. SNA-03 Fr.4 yielded **1** (31.0 mg) with a retention time of 25 min, while SNA-03 Fr.5 and CJA2-03 Fr.5 both yielded **2** (65 and 20 mg, respectively) with a retention time of 28 min (Figure S13, [Supporting Information](#)). Analytical NP-HPLC using a YMC Polyamine II column and conditions similar to those used for the final preparative separation showed that CJA2-03 Fr.4 contained a major component that eluted at the same retention time as that of SNA-03 Fr.4. However, the CJA2-03 Fr.4 material was lost during handling before final preparative purification could be achieved.

**NMR Analysis.** Fractions were characterized by 1D and 2D NMR spectroscopy using both D<sub>2</sub>O (99.99%) and DMSO-*d*<sub>6</sub> (99.99%). Purified compounds were dissolved in a minimum amount of D<sub>2</sub>O (99.99%), and the following spectra were recorded for both materials: <sup>1</sup>H, <sup>13</sup>C, DEPT (Figures 3 and 4; Figures S21–S28, Supporting Information), COSY, HSQC, HMBC, H2BC, NOESY, TOCSY, and HSQC-TOCSY (Figures S29–S36 and S40–S47, Supporting Information). A phase-sensitive COSY experiment was additionally carried out for **1** using a pulse program with the optimized 90 deg pulse of 11 μs and a relaxation time (d1) of 1 s (Figure S37, Supporting Information). Water suppression was applied to <sup>1</sup>H NMR spectra of pure compounds using standard procedures.

**Permethylolation.** Compounds **1** and **2** (200–500 μg of each) were permethylated as described previously<sup>54</sup> with modifications as follows. Base was freshly prepared using 4 mL of dry DMSO added to 100 μL of 50% NaOH (w/w), dried with repeated rinsing with DMSO, and dissolved in 2 mL of DMSO. Base (200 μL) was added to each carbohydrate sample and stirred briefly, after which iodomethane (100 μL) was added and the samples were stirred at room temperature for 40 min. The addition of base and iodomethane and stirring for 40 min was repeated and followed by addition of H<sub>2</sub>O (2 mL) to quench the reaction, yielding a cloudy solution. The remaining iodomethane was removed under a low flow of N<sub>2</sub>. The dried per-*O*-methylated carbohydrates were purified by solid-phase extraction (SPE; Sep-Pak C<sub>18</sub> 12 cc Vac Cartridge, 2 g). The SPE cartridge was conditioned with sequential aliquots of 10 mL each of MeOH and MeCN and 15 mL of H<sub>2</sub>O, in that order. The dried extracts were loaded onto the cartridge with H<sub>2</sub>O and eluted with MeCN. The samples were dried under N<sub>2</sub> prior to UHPLC/QTOF-ESIMS analysis using an Agilent Bonus RP18 (2.1 × 100 mm, 1.8 μm) column with a flow rate of 0.25 mL/min and a gradient of 3% MeOH(aq) to 100% MeOH over 5 min followed by isocratic elution with MeOH for 3 min. A 5 min wash with MeOH followed by an equilibration period of 13 min was completed between each run. The column temperature was set at 35 °C, and the injection volumes ranged from 3 to 5 μL, with all samples prepared in 1 mM NaOH in 50% MeOH(aq). Total ion chromatogram peaks were assigned according to the mass of the compounds. The conditions of the QTOFMS were as follows: ESI source with Jet Stream technology using a drying gas (N<sub>2</sub>) at 11.0 L/min and 250 °C; nebulizer, 35 PSIG, sheath gas at 10 mL/min and 325 °C; capillary, 3500 V; skimmer 65 V; Oct RF V, 750 V; fragmentor voltage, 100 V. The sample collision energy was set to 65 V. Samples were analyzed in ESI positive mode, and spectra were acquired across the range of *m/z* 100–1700 with accurate mass measurements obtained through the use of a reference ion correction using *m/z* 121.0509 (protonated purine) and 922.0098 [protonated hexakis(1*H*,1*H*,3*H*-tetrafluoropropoxy)phosphazine or HP-921]. The reference solution was introduced into the ESI source using a T-junction with an Agilent Series 1200 isocratic pump (Agilent Technologies, Santa Clara, CA, USA) containing a 100:1 splitter with a flow rate of 20 μL/min.

**Alditol Acetate Derivatization.** Alditol acetate derivatives of **1** and **2** were formed via hydrolysis, reduction with NaBD<sub>4</sub>, and *O*-acetylation. AA derivatives of the standards L-(+)-arabinose, D-(+)-glucose, L-(–)-xylose, D-(+)-fucose, L-(+)-rhamnose, D-(+)-galactose, and *myo*-inositol and of **1** and **2** were prepared individually using a modified version of a reported procedure.<sup>55</sup> Individual monosaccharide standards [100 μg each of L-(+)-arabinose, D-(+)-glucose, L-(–)-xylose, D-(+)-fucose, L-(+)-rhamnose, D-(+)-galactose] were combined with 20 μg of the internal standard, *myo*-inositol, in separate screw-cap tubes. A standard set of multiple monosaccharides (AAstd) was used to create a GC-MS calibration curve for quantification purposes and consisted of 50 μg each of L-(+)-arabinose, D-(+)-glucose, and L-(–)-xylose and 20 μg of *myo*-inositol. Compounds **1** and **2** (~100 μg each) were combined with 20 μg of *myo*-inositol in separate screw-cap tubes and were hydrolyzed via incubation in 2 M trifluoroacetic acid (TFA) at 121 °C for 2 h. 2-Propanol (200 μL) was added to the cooled samples followed by drying under N<sub>2</sub> while sitting in a water bath at 40 °C. The addition and subsequent drying of 2-propanol was repeated twice. Reduction

of the hydrolyzed glycosyl units was done in a solution of NaBD<sub>4</sub> (10 mg/mL) in 1 M NH<sub>4</sub>OH (200 μL) at room temperature overnight followed by neutralization with glacial HOAc in MeOH and drying. Any remaining NaBD<sub>4</sub> was removed by repeated addition and drying of MeOH/glacial HOAc (9:1). *O*-Acetylation was performed with Ac<sub>2</sub>O (250 μL) in TFA (99.9%, 230 μL) at 50 °C for 20 min. 2-Propanol was added to the cooled sample, and the mixture was dried. Na<sub>2</sub>CO<sub>3</sub> (0.2 M, 2 mL) was added and alditol acetate derivatives were extracted using CH<sub>2</sub>Cl<sub>2</sub> (2 mL). The extract was washed with H<sub>2</sub>O (2 × 1 mL) and concentrated to ~100 μL in preparation for GC-MS analysis.

Each sample (3 × 5 uL/injection) was separated on a Restek Rtx-2330 [30 m, 0.25 mm i.d., 0.2 μm film thickness (df)] column with an injector temp of 250 °C, a split ratio of 20:1, helium as the carrier gas, and a mass scan mode from *m/z* 50 to 500. An initial temperature of 80 °C was held for 2 min, with a first ramp at 30 °C/min to a final temperature of 170 °C and a second ramp at 4 °C/min to a final temperature of 240 °C, which was held for 20 min.

**Quantification of Alditol Acetate Derivatives.** In order to determine the relative molar quantities of each monomer in the oligosaccharides, a six-point calibration curve was created using the averaged peak areas (PA) from three injections of the standard (AA<sub>std</sub>). The detector response factor (RF; slope of the linear calibration curve) was used to calculate a relative response factor (RRF) of each monosaccharide standard (S) relative to the internal standard (IS), as follows:  $RRF = RF_S / RF_{IS}$ . The concentration (C) of each monosaccharide moiety (S) in the oligosaccharide samples was calculated using the corresponding standard monosaccharide RRF (e.g., the glucose RRF was used to calculate the concentration of glucose in the oligosaccharide sample) with the formula  $C_S = (C_{IS} \times PA_{S}) / (RRF_S \times PA_{IS})$ . The concentration of each monomeric moiety in the oligosaccharide sample was used to calculate the relative molar ratio of the monomers present. The concentration of the hexose moiety (glucose) was divided by its approximate molar mass of 180, and, likewise, the pentose moieties (arabinose and xylose) were divided by 150. The resulting values were compared to determine the relative molar ratio of each monomeric moiety.

**Partially Methylated Alditol Acetate Derivatization.** PMAA derivatives of **1** and **2** (400 μg each) were prepared using the permethylolation procedure as described above, immediately followed by the alditol acetate procedure. Derivatives were reduced to a volume of ~100 μL in CH<sub>2</sub>Cl<sub>2</sub> and analyzed by GC-MS, as described above. The ring size and linkage positions for the specific glycosyl moieties of **1** and **2** were determined using GC-MS via comparison of relative retention times (RRT; relative to the internal standard) to those of prepared PMAA monosaccharide standard derivatives (Table S5 and Section S1, Supporting Information). RRT data were combined with MS-fragmentation pattern information, and the identification of distinguishing mass fragments<sup>56</sup> was used to aid assignments due to the potential overlap of RRTs.

**Phenyl Thiocarbamate Derivatization.** Phenyl thiocarbamate derivatives of SNA-03 and the standards D-(+)-glucose, L-(+)-arabinose, D-(–)-arabinose, L-(–)-xylose, D-(+)-xylose, L-(+)-rhamnose, D-(+)-galactose, and D-(+)-mannose were formed as follows. Each sample (1 mg) was hydrolyzed in 2 M HCl for 1 h with stirring in an oil bath at 100 °C. Samples were neutralized by repeated addition of H<sub>2</sub>O and evaporation, and subsequent steps were performed as described previously.<sup>55</sup> The samples were cooled, and the retention times of the resulting optically active diastereoisomers derived from **1** and **2** were compared to those of the standards and a reagent blank by analytical scale HPLC using a Gemini C<sub>18</sub> (4.6 × 250 mm, 110 Å, 5 μm) column with a flow rate of 1 mL/min and a gradient of H<sub>2</sub>O (0.1% formic acid)/MeCN (90:10) to 100% MeCN over 45 min. A 5 min wash period with MeCN and a 15 min equilibration period were applied between each injection. The UV max plot and the UV absorbance at 210 nm were monitored, and each sample was injected twice to verify the retention times for each peak, with injection volumes of 2 μL for individual samples and standards and 3 μL for samples spiked with standards. An isocratic method with

a mobile phase of 27% MeCN(aq) was employed for samples spiked with L-(−)-xylose and L-(+)-arabinose.

**Antimicrobial Assays.** These assays were performed as a part of the antimicrobial screening program available at the National Center for Natural Products Research (NCNPR), at the University of Mississippi, according to previously reported methods<sup>57,58</sup> modified from the Clinical and Laboratory Standards Institute (CLSI) methods [formerly the National Committee for Clinical and Laboratory Standards (NCCLS)].<sup>59–62</sup> Samples tested included CJ, CJE, CJA, fraction SNA-03, and compound 2. All samples were tested against a panel of 10 pathogenic organisms including five fungi (*Candida albicans* ATCC 90028, *C. glabrata* ATCC 90030, *C. krusei* ATCC 6258, *Cryptococcus neoformans* ATCC 90113, and *Aspergillus fumigatus* ATCC 204305) and five bacteria (*Staphylococcus aureus* ATCC 29213, methicillin-resistant *S. aureus* ATCC 33591, *E. coli* ATCC 35218, *Pseudomonas aeruginosa* ATCC 27853, and *Mycobacterium intracellulare* ATCC 23068). Samples of CJ, CJE, and CJA were additionally tested against the protozoans *Plasmodium falciparum* (D6 clone) and *Leishmania donovani*. Amphotericin B served as the positive control for the *L. donovani* assay (producing 100% inhibition under the parameters used) and for the antifungal assay. Ciprofloxacin served as the positive control for bacterial pathogens. Percent growth inhibition was calculated relative to positive and negative controls, and samples were considered to be inactive if they produced growth inhibition of less than 50% (Table S6, Supporting Information). In the antibacterial and antifungal assays, CJ, CJE, and CJA samples were tested at a concentrations of 50 µg/mL; in the antiprotozoal assay these samples were tested at a concentration of 15.9 µg/mL against *P. falciparum* and at 80 µg/mL against *L. donovani*. SNA-03 was tested at concentrations of 200, 40, and 8 µg/mL, and compound 2 was tested at 20, 4, and 0.8 µg/mL.

**Breast Cancer Cell Viability Assay.** Breast cancer cells T47D and MDA-MB-231 were seeded into a 96-well culture plate at 30 000 cells per well and incubated at 37 °C for 24 h in 200 µL of 10% fetal bovine serum (FBS) DMEM/F12 medium supplemented with 50 µg/mL penicillin/streptomycin. Compounds 1 and 2 (100 µL) were added into separate wells at concentrations of 10, 30, and 100 µM. Fraction SNA-03 was added at 30 and 100 ppm. Samples were tested in triplicate. Chlorhexamide (CHX; 100 µL, 10 µM) was used as a positive control in addition to a medium control. The cultures were incubated at 37 °C for 48 h under normoxic conditions. The cells were fixed with 10% trichloroacetic acid for 1 h at 4 °C, washed four times with H<sub>2</sub>O, and allowed to air-dry. Sulforhodamine B (0.4%) in 1% HOAc was added, and samples were allowed to sit for 15 min at room temperature. The culture wells were washed four times with 1% HOAc and allowed to air-dry. Tris HCl buffer (200 µL, 10 mM) was added, and the plates were placed on a rotary table and vortexed for 5 min. Plates were read at 490/690 nm on a microplate reader. Percent inhibition was calculated as follows: % Inhibition =  $(1 - X_S)/(X_{ctrl})$ , where  $X_S$  is the average absorbance of the triplicate wells incubated with a sample and  $X_{ctrl}$  is the average absorbance of the triplicate media control wells (Table S7, Supporting Information).

**Escherichia coli-Uroepithelial Cell Antiadhesion Assay.** Samples were submitted to the EC-UEC antiadhesion assay while it was under development. A report of this assay has since been published.<sup>63</sup> Briefly, the procedure used for the submitted cranberry-derived samples was as follows: human uroepithelial cells (UEC; HTB-4) were seeded at  $1 \times 10^5$  cells per well in a 96-well culture plate and rinsed with phosphate-buffered saline (PBS). P-fimbriated *E. coli* (ATCC 700928) were subcultured in colony forming antigen (CFA) agar to promote expression of P-fimbriae<sup>64</sup> and incubated for 4 h at 35 °C with [<sup>3</sup>H]-uridine. The cells were rinsed with PBS and incubated with cranberry samples for 30 min at 35 °C. [<sup>3</sup>H]-*E. coli* and UECs were incubated together in a ratio of 400:1, respectively, for 1 h at 37 °C and washed with PBS. Radioactivity of the wells was measured by liquid scintillation.

Samples submitted included SNA, SNA-03, SNA-04, SNA-03 fractions Fr.1, Fr.3, Fr.4, Fr.5, Fr.6, Fr.7, Fr.8, Fr.9, and compounds 1 and 2. SNA-03-Fr.2 was not assayed due to sample loss during handling. Each sample was tested in duplicate along with a media

control, solvent control, and two positive controls (myricetin and a cranberry extract enriched for A-type proanthocyanidins; Figure S48, Supporting Information). Inhibition curves were collected with four concentration points, resulting in serial dilutions of the highest concentration attainable. The highest concentration tested varied depending on sample availability. The IC<sub>50</sub> value was calculated for positive controls but was unobtainable for cranberry samples (Section S2, Supporting Information).

**Heptasaccharide (1).** β-D-Glucopyranosyl-(1→4)-[α-D-xylopyranosyl-(1→6)]-β-D-glucopyranosyl-(1→4)-β-D-glucopyranosyl-(1→4)-[α-L-arabinofuranosyl-(1→2)]-α-D-xylopyranosyl-(1→6)]-β-D-glucopyranose: white, amorphous powder; moderately hygroscopic; <sup>1</sup>H and <sup>13</sup>C NMR data, Figures 3–5, Table 2, Figures S21, S22, S24, S25, S27, and S28 (Supporting Information); 2D NMR data, Figure 7, Figures S29–S37 (Supporting Information); QTOFESIMS of per-O-methylated compound (positive ion mode) [M + Na]<sup>+</sup> at m/z 1365.6545, indicative of a molecular formula of [C<sub>59</sub>H<sub>106</sub>O<sub>33</sub>Na]<sup>+</sup> (Figure S14, Supporting Information).

**Octasaccharide (2).** β-D-Glucopyranosyl-(1→4)-[α-L-arabinofuranosyl-(1→2)]-α-D-xylopyranosyl-(1→6)]-β-D-glucopyranosyl-(1→4)-β-D-glucopyranosyl-(1→4)-[α-L-arabinofuranosyl-(1→2)]-α-D-xylopyranosyl-(1→6)]-β-D-glucopyranose: white, amorphous powder; moderately hygroscopic; <sup>1</sup>H and <sup>13</sup>C NMR data, Figures 3, 4, and 6, Table 2, Figures S21, S23, S24, and S26–S28 (Supporting Information); 2D NMR data, Figures S40–S47 (Supporting Information); QTOFESIMS of per-O-methylated compound (positive ion mode) [M + Na]<sup>+</sup> at m/z 1525.7012, indicating a molecular formula of [C<sub>66</sub>H<sub>118</sub>O<sub>37</sub>Na]<sup>+</sup> (Figure S14, Supporting Information).

## ■ ASSOCIATED CONTENT

### Supporting Information

The Supporting Information is available free of charge on the ACS Publications website at DOI: 10.1021/acs.jnatprod.8b01044.

Complete NMR spectra of 1 and 2; additional tables and figures containing chromatographic, spectroscopic, and carbohydrate composition data; color images of the starting materials and an example Sephadex LH-20 separation with CJA material; further descriptions of the bioassay methods and results; additional discussion points (PDF)

## ■ AUTHOR INFORMATION

### Corresponding Authors

\*E-mail: cmcoleman4321@gmail.com.

\*Tel: +1 662-915-7144. E-mail: dferreir@olemiss.edu.

### ORCID

Christina M. Coleman: 0000-0001-5785-7425

Mei Wang: 0000-0003-3686-4292

Daneel Ferreira: 0000-0002-9375-7920

### Notes

The authors declare no competing financial interest.

## ■ ACKNOWLEDGMENTS

This project was funded in part by Ocean Spray Cranberries, Inc., Lakeville-Middleboro, MA, USA, for the isolation and structure elucidation of cranberry oligosaccharides and antiadhesion testing. Dr. C. Khoo, at Ocean Spray Cranberries, Inc., provided administrative assistance and coordinated initial contact between the University of Mississippi and Washington State University for antiadhesion bioassay testing. Various resources within the National Center for Natural Products Research (NCNPR) at the University of Mississippi were made available by Dr. I. Khan, including access to

antimicrobial testing, performed by Ms. M. Wright, and to breast cancer cell viability testing, performed by Ms. F. Mahdi. Funding for antimicrobial testing was provided in part by USDA Agricultural Research Service, Specific Cooperative Agreement No. 58-6408-1-603 (antibacterial and antiprotozoal assays) and in part by the NIH, NIAID, Division of AIDS grant number AI 27094 (antifungal assay). Analytical and preparative HPLC-ELSD equipment was made available by Dr. J. Williamson and Dr. S. J. Cutler in the Department of Medicinal Chemistry, School of Pharmacy, University of Mississippi. The Complex Carbohydrate Research Center, University of Georgia, Athens, GA, provided training for K.M.A., general information, and support for derivatization techniques. Dr. J. Parcher, in the Department of Chemistry and Biochemistry at the University of Mississippi, assisted with GC-MS analytical procedures.

## ■ DEDICATION

Dedicated to Dr. Rachel Mata, of the National Autonomous University of Mexico, Mexico City, Mexico, and to Dr. Barbara N. Timmermann, of the University of Kansas, for their pioneering work on bioactive natural products.

## ■ REFERENCES

- (1) Smith, T.; Kawa, K.; Eckl, V.; Stredney, R. *Herbalgram* **2017**, *115*, 56–65.
- (2) Blumberg, J. B.; Camesano, T. A.; Cassidy, A.; Kris-Etherton, P.; Howell, A. B.; Manach, C.; Ostertag, L. M.; Sies, H.; Skulas-Ray, A.; Vita, J. A. *Adv. Nutr.* **2013**, *4*, 618–632.
- (3) Pappas, E.; Schaich, K. M. *Crit. Rev. Food Sci. Nutr.* **2009**, *49*, 741–781.
- (4) Zafriri, D.; Ofek, I.; Adar, R.; Pocino, M.; Sharon, N. *Antimicrob. Agents Chemother.* **1989**, *33*, 92–98.
- (5) Ofek, I.; Goldhar, J.; Zafriri, D.; Lis, H.; Adar, R.; Sharon, N. *N. Engl. J. Med.* **1991**, *324*, 1599.
- (6) Ofek, I.; Goldhar, J.; Sharon, N. *Adv. Exp. Med. Biol.* **1996**, *408*, 179–183.
- (7) Burger, O.; Ofek, I.; Tabak, M.; Weiss, E. I.; Sharon, N.; Neeman, I. *FEMS Immunol. Med. Microbiol.* **2000**, *29*, 295–301.
- (8) Rafsanjany, N.; Senker, J.; Brandt, S.; Dobrindt, U.; Hensel, A. J. *Agric. Food Chem.* **2015**, *63*, 8804–8818.
- (9) Neto, C. C.; Penndorf, K. A.; Feldman, M.; Meron-Sudaim, S.; Zakay-Rones, Z.; Steinberg, D.; Fridman, M.; Kashman, Y.; Ginsburg, I.; Ofek, I.; Weiss, E. I. *Food Funct.* **2017**, *8*, 1955–1965.
- (10) Weiss, E. I.; Hourri-Haddad, Y.; Greenbaum, E.; Hochman, N.; Ofek, I.; Zakay-Rones, Z. *Antiviral Res.* **2005**, *66*, 9–12.
- (11) Tipton, D. A.; Christian, J.; Blumer, A. *Arch. Oral Biol.* **2016**, *68*, 88–96.
- (12) Howell, A. B.; Der Marderosian, A.; Foo, L. Y. *N. Engl. J. Med.* **1998**, *339*, 1085–1086.
- (13) Foo, L. Y.; Lu, Y.; Howell, A. B.; Vorsa, N. *J. Nat. Prod.* **2000**, *63*, 1225–1228.
- (14) Coleman, C. M. *Cranberry Metabolites With Urinary Anti-Adhesion Activity*. Ph.D. Dissertation, University of Mississippi, University, MS, 2014.
- (15) Coleman, C. M.; Auken, K. M.; Killday, K. B.; Azadi, P.; Black, I.; Ferreira, D. *J. Nat. Prod.* **2019**, *82*, DOI: 10.1021/np8b01043.
- (16) Hotchkiss, A. T.; Nunez, A.; Strahan, G. D.; Chau, H. K.; White, A. K.; Marais, J. P. J.; Hom, K.; Vakkalanka, M. S.; Di, R.; Yam, K. L.; Khoo, C. *J. Agric. Food Chem.* **2015**, *63*, 5622–5633.
- (17) Sun, J.; Marais, J. P. J.; Khoo, C.; LaPlante, K.; Vejborg, R. M.; Givskov, M.; Tolker-Nielsen, T.; Seeram, N. P.; Rowley, D. C. *J. Funct. Foods* **2015**, *17*, 235–242.
- (18) Holmes, A. B.; Rha, C. *J. Food Sci.* **1978**, *43*, 112–115.
- (19) Marlett, J. A.; Vollendorf, N. W. *Food Chem.* **1994**, *51*, 39–44.
- (20) Turi, C. E.; Finley, J.; Shipley, P. R.; Murch, S. J.; Brown, P. N. *J. Nat. Prod.* **2015**, *78*, 953–966.
- (21) Sun, J.; Liu, W.; Ma, H.; Marais, J. P. J.; Khoo, C.; Dain, J. A.; Rowley, D. C.; Seeram, N. P. *J. Berry Res.* **2016**, *6*, 149–158.
- (22) Ozcan, E.; Sun, J.; Rowley, D. C.; Sela, D. A. *Appl. Environ. Microbiol.* **2017**, *83*, e01097–17.
- (23) Blumberg, J. B.; Basu, A.; Krueger, C. G.; Lila, M. A.; Neto, C. C.; Novotny, J. A.; Reed, J. D.; Rodriguez-Mateos, A.; Toner, C. D. *Adv. Nutr.* **2016**, *7*, 759S–770S.
- (24) Oakley, E. T.; Magin, D. F.; Bokelman, G. H.; Ryan, W. S. J. *Carbohydr. Chem.* **1985**, *4*, 53–66.
- (25) Reis, A.; Domingues, M. R. M.; Domingues, P.; Ferrer-Correia, A. J.; Coimbra, M. A. *Carbohydr. Res.* **2003**, *338*, 1497–1505.
- (26) Fredriksson, S.-A.; Nilsson, B. *Adv. Mass Spectrom.* **1998**, *14*, C025930/1.
- (27) Cancilla, M. T.; Penn, S. G.; Carroll, J. A.; Lebrilla, C. B. *J. Am. Chem. Soc.* **1996**, *118*, 6736–6745.
- (28) Whiton, R. S.; Lau, P.; Morgan, S. L.; Gilbert, J.; Fox, A. J. *Chromatogr.* **1985**, *347*, 109–20.
- (29) Tanaka, T.; Nakashima, T.; Ueda, T.; Tomii, K.; Kouno, I. *Chem. Pharm. Bull.* **2007**, *55*, 899–901.
- (30) Duus, J. O.; Gotfredsen, C. H.; Bock, K. *Chem. Rev.* **2000**, *100*, 4589–4614.
- (31) Islam, S. M.; Richards, M. R.; Taha, H. A.; Byrns, S. C.; Lowary, T. L.; Roy, P. N. *J. Chem. Theory Comput.* **2011**, *7*, 2989–3000.
- (32) Sudjaroen, Y.; Hull, W. E.; Erben, G.; Wuertele, G.; Changbumrung, S.; Ulrich, C. M.; Owen, R. W. *Phytochemistry* **2012**, *77*, 226–37.
- (33) Wyman, C. E.; Decker, S. R.; Himmel, M. E.; Brady, J. W.; Skopec, C. E.; Viikari, L. In *Polysaccharides: Structural Diversity and Functional Versatility*, 2nd ed.; Dumitriu, S., Ed.; CRC Press/Marcel Dekker: New York, 2005; pp 1023–1062.
- (34) Waldron, K. W.; Faulds, C. B. In *Comprehensive Glycoscience, from Chemistry to Systems Biology, Vol. 1; Introduction to Glycoscience; Synthesis of Carbohydrates*; Kamerling, J. P.; Boons, G. J.; Lee, Y. C.; Suzuki, A.; Taniguchi, N.; Voragen, A. G. J., Eds.; Elsevier: Boston, 2007; pp 181–201.
- (35) Brummell, D. A.; Dal Cin, V.; Crisosto, C. H.; Labavitch, J. M. *J. Exp. Bot.* **2004**, *55*, 2029–2039.
- (36) Goulão, L. F.; Oliveira, C. M. *Trends Food Sci. Technol.* **2008**, *19*, 4–25.
- (37) York, W. S.; Kumar Kolli, V. S.; Orlando, R.; Albersheim, P.; Darvill, A. G. *Carbohydr. Res.* **1996**, *285*, 99–128.
- (38) Coleman, C. M.; Akgul, Y.; Kimble, L. L.; Mathison, B. D.; Chew, B. P.; Ferreira, D. *Phytochem. Anal.*, 2019, in preparation.
- (39) Weh, K. M.; Clarke, J.; Kresty, L. A. *Antioxidants* **2016**, *5*, 27/1–27/20.
- (40) Vu, K. D.; Carlettini, H.; Bouvet, J.; Cote, J.; Doyon, G.; Sylvain, J. F.; Lacroix, M. *Food Chem.* **2012**, *132*, 959–967.
- (41) Cote, J.; Caillet, S.; Doyon, G.; Dussault, D.; Sylvain, J. F.; Lacroix, M. *Food Control* **2011**, *22*, 1413–1418.
- (42) Das, Q.; Islam, M. R.; Marcone, M. F.; Warriner, K.; Diarra, M. S. *Food Control* **2017**, *73*, 650–662.
- (43) Tuomivaara, S. T.; Yaoi, K.; O'Neill, M. A.; York, W. S. *Carbohydr. Res.* **2015**, *402*, 56–66.
- (44) Holck, J.; Hotchkiss, A. T.; Meyer, A. S.; Mikkelsen, J. D.; Rastall, R. A. In *Food Oligosaccharides: Production, Analysis and Bioactivity*; Moreno, F. J.; Luz Sanz, M., Eds.; John Wiley & Sons: New York, 2014; pp 76–87.
- (45) Bode, L. *Early Hum. Dev.* **2015**, *91*, 619–622.
- (46) Rudloff, S.; Pohlentz, G.; Borsch, C.; Lentze, M. J.; Kunz, C. B. *Br. J. Nutr.* **2012**, *107*, 957–963.
- (47) Umemura, M.; Yuguchi, Y. *Cellulose* **2009**, *16*, 361–371.
- (48) Umemura, M.; Yuguchi, Y. *Carbohydr. Res.* **2005**, *340*, 2520–2532.
- (49) Haard, N. F.; Chism, G. W. In *Food Chem.*; Fennema, O. R., Ed.; Marcel Dekker, Inc.: New York, 1996; pp 943–1012.
- (50) Robyt, J. F. *Essentials of Carbohydrate Chemistry*; Springer-Verlag: New York, NY, 1998.

- (51) Wang, J.; Chen, C.; Yu, Z.; He, Y.; Yong, Q.; Newburg, D. S. *Eur. Food Res. Technol.* **2017**, *243*, 133–146.
- (52) Katouli, M. *Iran J. Microbiol.* **2010**, *2*, 59–72.
- (53) Rossez, Y.; Holmes, A.; Lodberg-Pedersen, H.; Birse, L.; Marshall, J.; Willats, W. G. T.; Toth, I. K.; Holden, N. J. *J. Biol. Chem.* **2014**, *289*, 34349–34365.
- (54) Ciucanu, I.; Kerek, F. *Carbohydr. Res.* **1984**, *131*, 209–217.
- (55) Whiton, R. S.; Lau, P.; Morgan, S. L.; Gilbert, J.; Fox, A. J. *Chromatogr.* **1985**, *347*, 109–120.
- (56) Jansson, P. E.; Kenne, L.; Liedgren, H.; Lindberg, B.; Lönngrén, J. *Chem. Commun. (Stockholm Univ.)* **1976**, *8*, 1–75.
- (57) Zhang, J. R.; Aziz, A.; Jain, S.; Jacob, M. R.; Khan, S. I.; Tekwani, B. L.; Ilias, M. *Res. Rep. Med. Chem.* **2012**, *2*, 1–6.
- (58) Rahman, A. A.; Samoylenko, V.; Jacob, M. R.; Sahu, R.; Jain, S. K.; Khan, S. I.; Tekwani, B. L.; Muhammad, I. *Planta Med.* **2011**, *77*, 1639–1643.
- (59) NCCLS. *Reference Method for Broth Dilution Antifungal Susceptibility Testing of Yeasts; Approved Standard M27-A2*; National Committee on Clinical Laboratory Standards, 2002.
- (60) NCCLS. *Methods for Dilution of Antimicrobial Susceptibility Tests for Bacteria that Grow Aerobically, Approved Standard*, Seventh ed.; National Committee on Clinical Laboratory Standards, 2006.
- (61) NCCLS. *Susceptibility Testing of Mycobacteria, Nocardia, and Other Aerobic Actinomycetes; Tentative Standard-Approved Standard, M24-A*; National Committee on Clinical Laboratory Standards, 2003.
- (62) NCCLS. *Reference Method for Broth Dilution Antifungal Susceptibility Testing of Filamentous Fungi; Approved Standard, M38-A*; National Committee on Clinical Laboratory Standards, 2002.
- (63) Mathison, B. D.; Kimble, L. L.; Kaspar, K. L.; Khoo, C.; Chew, B. P. *J. Nat. Prod.* **2013**, *76*, 1605–1611.
- (64) Evans, D. G.; Evans, D. J.; Tjoa, W. *Infect. Immun.* **1977**, *18*, 330–337.